2016

Spatial-Temporal Stochasticity of Electric Vehicles in Integrated Traffic and Power System

Sadhana Shrestha
South Dakota State University, sadhana.shrestha@sdstate.edu

SPATIAL-TEMPORAL STOCHASTICITY OF ELECTRIC VEHICLES IN INTEGRATED TRAFFIC AND POWER SYSTEM

BY

SADHANA SHRESTHA

A thesis submitted in partial fulfillment of the requirements for the

Master of Science

Major in Electrical Engineering

South Dakota State University

2016

SPATIAL-TEMPORAL STOCHASTICITY OF ELECTRIC VEHICLES IN INTEGRATED TRAFFIC AND POWER SYSTEM

This thesis is approved as a creditable and independent investigation by a candidate for the Master of Science in Electrical Engineering degree and is acceptable for meeting the thesis requirements for this degree. Acceptance of this thesis does not imply that the conclusions reached by the candidates are necessarily the conclusions of the major department.

Timothy Hansen, PhD
Major/Thesis Advisor Date

Steven Hietpas, PhD
Head, Electrical Engineering and Computer Science Date

Dean, Graduate School Date

ACKNOWLEDGEMENTS

I would like to express my deep gratitude to my supervisor Dr. Timothy M. Hansen for his guidance, support, and encouragement. He was very generous on providing his invaluable advice both in research and my career. Every discussion on research with him was very encouraging and fruitful, which always broadened my knowledge. I would also like to thank Dr. Reinaldo Tonkoski and Dr. Zhen Ni for agreeing to serve as my thesis committee members. I appreciate their invaluable suggestions while reviewing this thesis. I would also like to express my special thanks to Dr. David Galipeau and Dr. Qiquan Qiao for their support during my course of study.

I am also thankful to South Dakota State University, Department of Electrical Engineering and Computer Science for providing me necessary resources for conducting this research. I would like to express my gratitude to all the staff and faculty members of this department for their help and encouragement.

I would like to thank my parents, my brother Shakti Shrestha, my sister Salina Shrestha and brother in-law Suyash Shrestha for their unconditional love and support. I could not have done it without them.

I would also like to thank my friend Dipesh Shrestha for his help and support. I really appreciate his willingness to discuss about this research and make this work interesting. Finally, I would like to express my sincere acknowledgement to all my friends at South Dakota State University for their company and support which made my life at Brookings so pleasant.

CONTENTS

ABBREVIATIONS

BEV	Battery Electric Vehicle
DOD	Depth of Discharge
EPRI	Electric Power Research Institute
EREV	Extended Range Electric Vehicles
EV	Electric Vehicle
IC	Integrated Circuit
ICE	Internal Combustion Engine
NHTS	National Household Travel Survey
PHEV	Plugged-in Hybrid Electric Vehicle
RBTS	Roy Billinton Test System
SOC	State of Charge
V2G	Vehicle to Grid

LIST OF FIGURES

LIST OF TABLES

ABSTRACT

SPATIAL-TEMPORAL STOCHASTICITY OF ELECTRIC VEHICLES IN INTEGRATED TRAFFIC AND POWER SYSTEM

SADHANA SHRESTHA

2016

A penetration of a large number of electric vehicles for charging their batteries in the grid can have a negative impact to the grid. To prevent a negative effect to the grid, the behavior of electric vehicles must be accurately modeled and their charging schedules must be coordinated. Therefore, it is necessary to determine where and how much charge is available in electric vehicles in the distribution system. In this thesis, a state transition algorithm is designed to determine a stochastic model of electric vehicles to simulate electric vehicle movement in an integrated traffic and power network. Dijkstra's algorithm is used to determine the shortest distance between end-user residential and office areas. An uncoordinated and semi-coordinated charging technique are used to charge electric vehicles at different time intervals at different charging stations based on their driving patterns. Monte Carlo simulation is performed to analyze the effect of uncertainty in driving behavior. Results show that uncoordinated charging techniques generate new peaks in the load profile of each node in the distribution system and cause undervoltage problems in the power network. The semi-coordinated charging technique introduces a delay in the charging time to shift electric vehicle charging loads to off-peak times. Hence, with the semi-coordinated charging method, it is unnecessary to immediately upgrade the distribution network infrastructure to avoid network overloading.

CHAPTER 1 INTRODUCTION

1.1 Background

The usage of conventional internal combustion engine (ICE) vehicles contribute to a large amount of greenhouse gas emissions and air pollution globally. In USA, 27 percent of global warming pollution is caused by the use of gasoline in vehicles [1]. The global concern about the environmental change, rise in price of gasoline products, and depletion of fossil fuels have increased the adoption of electric vehicles (EVs) [2]. EVs are gaining popularity as environmentally friendly transportation due to their high energy efficiency and low CO_2 emissions compared to conventional vehicles. The surplus of electricity generated from renewable energy sources can also be considered as a driving force behind the widespread adoption of EVs. Moreover, EVs have a fast response and can act as either a source or generator for Vehicle to Grid (V2G) services. There are different EVs like Tesla, Nissan Leaf, Chevrolet Volt, Faraday Future, etc., which are trying to commercialize in the vehicle industry. One of the largest EVs developed by Tesla is "Tesla roadster" that can drive 350 kilometers with maximum speed 210 kmph [3]. In the US, it is expected that the sales of EVs will reach to 12 percent of all registered vehicles by 2025 [4].

From a distribution planning perspective, EVs are an unknown quantity representing potential demand that varies both spatially (with respect to space) and temporally (with respect to time) across the system [5]. To analyze the impact of EVs charging load on the electric grid, information regarding spatial and temporal distribution of EVs is required. Due to movement of EVs from one location to another at different time intervals, the total

number of EV batteries available for charging at any charging station varies with respect to time. Moreover, there exists uncertainty in EV users' driving behavior. The driving behavior depends on arrival time, departure time, driving speed, driving distance, parking duration, battery capacity of each EV, road condition, etc. This randomness adds additional complexity in determining the available number of EVs, but this will make accurate prediction of amount of electricity consumed by EV batteries and their state of charge. Therefore, modeling of EVs needs to be performed considering the complexity related with the use of EVs [6].

EVs affect both the traffic and power system. EVs use the traffic network to travel from one location to another [7]. Energy stored in EV batteries are consumed when they move in the traffic network. The available battery capacity of EV is inversely proportional to the total distance traveled. Hence, proper analysis of movement of EVs among various streets in the traffic network is important. Once the locations of EVs are known, information regarding amount of energy required to charge them at the respective nearest charging station can be calculated. EVs are connected to the grid to charge their batteries. At the end of the day, they are parked for longer time at home. So, charging stations are installed usually at parking lot of home by utility companies. A normal socket or dedicated charging socket is available to charge EVs through 120V (Level-1) or a 240V (Level-2) voltage supply at residential node. Penetration of EVs may not affect transmission system since large generators are available in power system to balance deficient loads, but these may adversely affect small distribution networks. Especially, in low ($\leq$ 1 kV) and medium voltage level distribution systems (1 kV $-$ 36 kV), EV charging loads add more stress.

With an increase in penetration of EVs in the grid, planning and operation of

distribution system becomes more complicated. Lots of EVs means a large amount of electricity demand. Most of the EV owners will arrive home from work within narrow time space and charge them as soon as they reach home. The grid is congested mostly in the evening due to their own residential load profile. Charging of EVs at the same time adds more burden to the already congested grid. This uncontrolled and random charging can cause additional peak in the system load profile, causing severe voltage fluctuations, increase in system losses, and decrease in the system efficiency in the distribution network [4]. This results in the overheating of the equipment and leads to the failure of loads. In long term, it may lead to blackout. To solve these issues, the capacity of transformers and lines in distribution network may be increased, but at significant cost. On the other hand, the simplest way to reduce stress in the grid during peak time is not to charge EVs during that time or charge them at different nodes due to the fact that EVs charging time can be controlled. Scheduling of charging of EVs at different charging time appears more realistic than at different charging stations because the charging stations for a particular house is fixed. However, EVs are parked at office for about 7 hours on average [8]. Also, solar power is available abundantly during the middle of the day. Thus, charging at the office can also be a convenient way to recharge EVs. If EVs are fully charged at the office, then EV charging demands are reduced at home at night. Additionally, the charging behavior may be influenced more by the electricity price during the different hours of a day. The price of electricity is highest during the peak hour period.

Several charging techniques, such as off-peak charging technique, coordinated charging scheme, and smart charging techniques can be applied for EV charging to shift loads in the middle of night when the cost of electricity is low or during day time when

solar energy sources can be used to charge EVs [9]. Off-peak charging technique is one of the simplest charging technique that can potentially reduce the addition of EVs load at peak time, thus deferring any immediate upgrade in their generation, transmission, and distribution infrastructure. However, simply shifting EV loads by constant time may cause simultaneously charging of multiple EV loads, causing even higher increase in peak load demand and additional voltage drops [10]. So, EV charging loads have to be shifted randomly based on their arrival time and departure time to flatten the load profile. Monte Carlo simulations need to be performed to analyze the uncertainties related with use of EVs [11]. Monte Carlo simulation helps to take better decision by analyzing many possible outcomes.

In this thesis, the load profile of the distribution system is flattened by using semi-coordinated charging technique. Demand side management is performed to solve the aforementioned problems of EVs in the distribution system.

1.2 Previous Work

Many studies have been conducted related to EVs assuming large penetration of EVs in future grid. Simpson et al. in 2006 analyzed the benefits of using EVs for customers. They found that the future penetration of EVs are affected by the cost and life of EVs and their batteries. They concluded that EVs can save up to 45% per vehicle petroleum consumptions that supports use of EVs in future [12]. Electric Power Research Institute (EPRI) in 2007 studied the environmental impacts of EVs. They found that EVs penetration can reduce CO_2 emissions from 25% to 85% by 2050 based on different scenarios [13]. Rezai et al. in 2012 examined the impact of uncoordinated charging in the

rural distribution system of Canada. They used fast and slow charging technique for EV charging. They concluded that less than 15% of EV penetration is permissible if fast charging technique is used, and less than 25% if slow charging method is applied [14].

Clement et al. in 2010 developed coordinated charging technique with the objective of minimizing power loss and maximizing grid load factor. They assumed that EVs will arrive home between 6 pm to 9 pm and at office at 10 am. They considered fixed period for charging EVs, which is not practical [4]. Qian et al. in 2010 determined EV charging load based on uncontrolled, controlled, and smart charging technique. They found out that the smart charging technique provides maximum benefit to the customer and utility operator. However, they have assumed that all EVs are charged from fixed starting time at home and office. They have also considered the same load profile in residential and commercial areas that is unrealistic [10].

Fernandez et al. in 2011 proposed a technique to examine the impact of different level of EV penetration in distribution system design. They found that energy loss in the system may rise up to 40% with maximum EV penetration. The cost of distribution system that can tolerate a maximum EV penetration are found to be around 15% higher than network with no EV penetration. However, they have not considered distribution of EVs at different time interval while modeling EV charging load [15]. Taylor et al. in 2010 used real world driving data from National House Travel Survey (NHTS) to generate pattern of EV arriving at home in a day. They assumed that EV charging loads follow the pattern of arrival time distribution. But, they have not controlled the duration for which EVs are connected to the grid for charging. They also used controlled charging technique in order to shift EV charging load during off-peak hour by adding constant time delay.

However, it creates another peak in the system. They have not considered the randomness in driving behavior [16].

Lee et al. in 2012 used real world driving data obtained from the survey conducted by University of Michigan Transportation Research Institute to develop temporal distribution of arrival and departure time. They proposed statistical modeling approach to generate realistic driving pattern. The driving patterns are randomly assigned to the spatial temporal model of EVs. However, they have not use Monte Carlo methods to analyze the randomness in the driving behavior [17]. Lojowska et al. in 2012 used Copula distribution to derive relationship between arrival time, departure time, and distance traveled. They also used two charging technique to derive EV charging load, i.e., uncontrolled charging method and controlled charging technique with charging time represented by uniform distribution with interval between arrival and departure time. The driving distances are represented by random probability distribution function. However, they did not consider traffic network to determine the route EVs follow [9].

Tang et al. in 2016 developed probabilistic model of nodal EV charging demand. EVs are assumed to move with respect to time and space in an integrated traffic and power network. Random trip chains are considered to model randomness in driving behavior. However, they have not done power flow analysis to observe the effects of nodal EV charging loads in power system. Only uncoordinated charging technique is applied in this work. The modeling of EV also did not account for randomness in driving speed of EV users [7].

No work has been done to analyze the impact of nodal EV charging load network considering EV model developed taking into account realistic driving pattern and EV

movement in integrated traffic and power network.

1.3 Motivation

The main motivation for this work is due to the need to decrease the negative impact of EVs in distribution system by considering spatial-temporal behavior of EVs as a distributed storage system. The hypothesis for this study is that demand side management using off–time charging technique will smoothen the load profile of various systems and maintain the voltage within permissible limits.

1.4 Objective

The objective of this thesis is to determine EV charging loads based on spatial temporal model of EV and use different charging technique to examine the impact charging load on various nodes of distribution system. The specific tasks of this research were to:

1) Develop model of integrated traffic and power network based on Bus 5 distribution system of Roy Billinton Test System (RBTS) [7];

2) Modeling of EV users driving pattern;

3) Use several charging techniques for charging EVs at different locations; and

4) Use Monte Carlo simulation to analyze nodal voltage profile with addition of EV charging load in RBTS Bus 5.

The tasks performed will determine EV charging loads at various nodes with respect to time and space when different charging techniques are used. Moreover, this study will

determine the importance of demand side EV charging load management for improving the nodal voltage profile.

1.5 Contributions

The major contributions of this work are:

1) Addition of realistic driving patterns in an integrated traffic and electric power network considering randomness in driving behavior;

2) Use of Dijkstra's algorithm to determine shortest driving distance between residential and commercial nodes;

3) Develop state transition algorithm to calculate number of EVs at different nodes; and

4) Use Monte Carlo simulations and semi-controlled charging techniques to eliminate voltage problems in distribution system due to EV charging loads.

1.6 Thesis Outline

This thesis has been organized as follows: Chapter 2 describes the concept of EVs, Dijkstra's algorithm, different charging techniques, and RBTS Bus 5 distribution network. Chapter 3 introduces the procedure to develop and implement Dijkstra's algorithm in integrated traffic and power network, and use of Monte Carlo simulation for load flow analysis. It describes about system model used for purpose of simulation. Chapter 4 presents the simulation results and analysis. Finally, Chapter 5 presents the conclusions, limitations, and possible future work.

CHAPTER 2 THEORY

Chapter 2 provides detailed information on EVs, battery technologies used in EVs and EV battery charging techniques. Graph theory and Dijkstra's algorithm are also explained in detail. Theories related to distribution network, load flow analysis, and Monte Carlo simulations are also presented.

2.1 Electric Vehicles (EVs)

EVs are those vehicles which are powered completely or partially by using electricity. EVs consist of several parts such as battery, electric motor, generator, mechanical transmission, and power control system. Batteries are used to store the energy. EVs are driven by one or more electric motors that are powered by rechargeable batteries. The first four- wheel EV was developed by William Morrison in 1830 with non-rechargeable batteries [18]. Since then, there has been huge progress in development of EV technology. The range of distance that can be traveled by fully charged EVs are shorter than that of conventional gas/diesel fueled vehicles. The distance that EVs can travel varies with speed, driving style, and geographical features of driving locations. However, according to U.S. Department of Transportation Federal Highway Administration, this range is enough for more than 90% of all household vehicle trips in U.S. [19].

The advantages of using EVs as compared to conventional ICE based vehicles are described below.

1) Energy Efficient: EVs are highly efficient as compared to conventional ICE vehicles.

EVs convert 59%-62% of energy from grid to power wheel while conventional vehicles convert only 17%-21% of total energy.

2) Environmentally Friendly: EVs are not responsible for producing any pollutants. Power plants that generate electricity for EVs may emit harmful gases, but renewable energy sources such as solar, wind, etc., can be used to charge batteries. These renewable sources do not cause any pollution to the environment.

3) Performance Benefits: EVs need less maintenance. They operate quietly as compared to conventional vehicles.

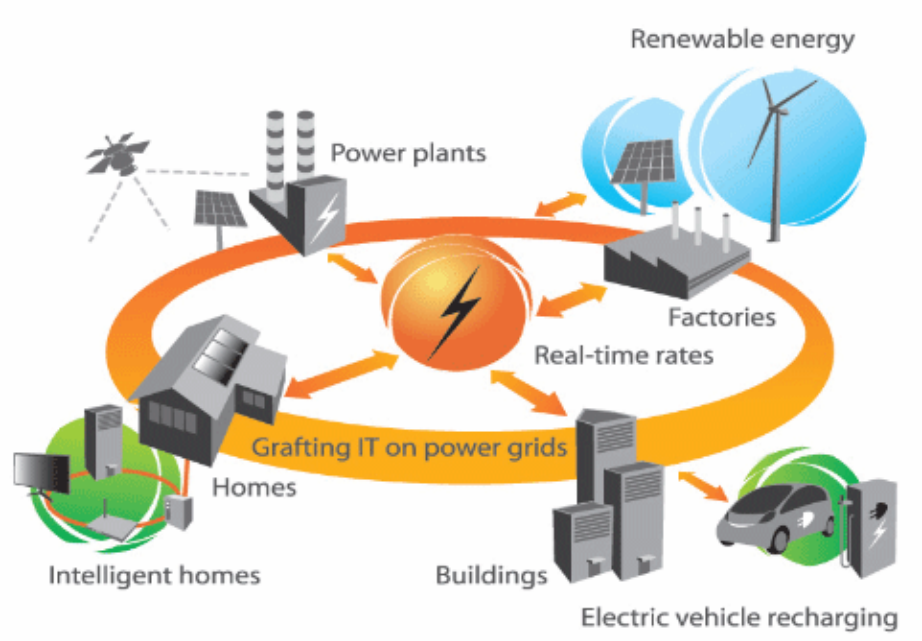

Figure 2.1. Integration of EVs to Distribution Network [20]

2.1.1 Classification of EVs

EVs are classified baesd on their size, battery capacities and charging method. The three major types of EVs are described below:

2.1.1.1 Plug-in Hybrid Electric Vehicles

Plug-in Hybrid Electric Vehicles (PHEV) are those vehicles that may be powered by conventional fuel such as gasoline, oil, etc., or electric energy stored in a battery. Due to the storage of energy in PHEV battery, it can reduce the consumption of gasoline under typical driving condition. Since electricity is cleaner source of energy, PHEV emits less greenhouse gases as compared to conventional vehicle. Chevy Volt, Ford Fusion Energi, etc. are the examples of PHEVs.

2.1.1.2 Extended Range Electric Vehicles

Extended Range Electric Vehicles (EREVs) are those vehicles with internal combustion engine and larger battery bank of size 16-27 kWh. The ICE coupled with the battery provides large driving range by recharging the battery whenever required. Electric motor turns the wheel while gasoline engine generates electricity needed to power electric motor. EREVs can run without using gasoline until the battery needs recharging. Toyota Prius, BMW i3, etc., are examples of EREVs.

2.1.1.3 Battery Electric Vehicles

Battery Electric Vehicles (BEVs) are those vehicles that use chemical energy stored in rechargeable battery packs. Batteries are charged by plugging into an outlet or charging station. BEV has electric motors and motor controllers instead of ICE for the purpose of propulsion. These vehicles never produce tailpipe emissions and have longer driving range as compared to PHEVs. Nissan LEAF, Ford Focus Electric, etc. are some of the examples of BEVs.

2.1.2 Battery Technologies

Secondary or rechargeable batteries are the energy storage devices used in EVs. Electric battery are the combination of two or more electric cells connected together. DC electricity is generated due to chemical reaction between electrodes and electrolyte. The requirement of the battery varies with the type of EV. While discharging, circuits are closed due to connection of electrochemical cell with load. Electrons move from anode through load to cathode. During charging, electrons flow in opposite direction creating potential difference between electrochemical cell. The most common type of battery used in EVs are explained below.

2.1.2.1 Lead Acid Battery

Lead acid battery is one of the oldest and most popular battery technology. It uses lead and lead dioxide as electrode. It is popular due to its low cost and large power to weight ratio. It is commonly used for the purpose of starter, lightning and ignition in traditional cars. The main drawbacks of this battery is low energy density and restricted lifetime.

2.1.2.2 Nickel Cadmium Battery

Nickel cadmium battery uses nickel oxyhydroxide and metallic cadmium as electrodes. It has higher specific energy content as compared to lead acid batteries. It is more tolerant to deep charging and has higher power density. Since cadmium is toxic in nature and memory effect reduce cell voltage, this battery is not used widely.

2.1.2.3 Nickel Metal Hydride Battery

Nickel metal hydride battery uses nickel cadmium cell and hydrogen absorbing alloy as electrodes. It has higher energy and power density as compared to nickel cadmium battery. It has good cycle life and is less toxic in nature.

2.1.2.4 Lithium Ion Battery

Lithium ion battery is one of the most promising battery that uses intercalated lithium compound as electrode material. Since lithium is lightest metal, it has greatest potential for electrochemical reaction. It provides largest energy density for weight. The cells are very tolerant of reverse currents, deep discharge, and high drain rate. However, it is fragile and requires a protection circuit to operate safely. The battery subjects to ageing if not used and frequently fails after two-three years.

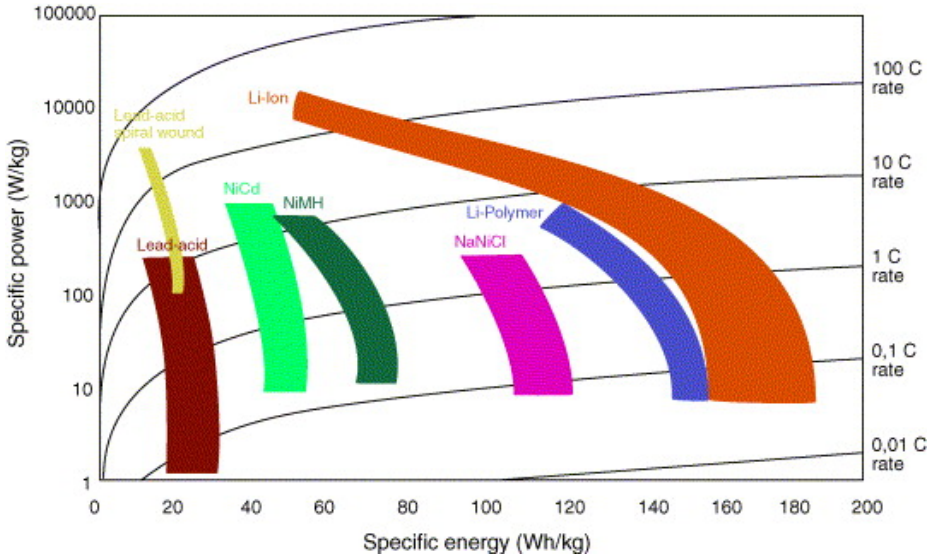

Figure 2.2. Comparison of performance of different battery technologies [21]

Figure 2.2 shows the specific energy and power of different battery based at various rated capacities. C-rate means the rate at which battery is being discharged in terms of its

rated capacity. 10 C-rate means the battery will become fully discharged in 10 hours. The traditional rechargeable battery type used in EVs is the lead-acid battery. However, other batteries are also gaining popularity in modern EVs. In this thesis, EVs are assumed to have lithium ion battery.

Table 2.1 shows the type of battery used by several EVs manufacturing companies.

Table 2.1. Batteries used in EVs of selected car manufacturers [22]

Company	**Country**	**Vehicle Model**	**Battery Technology**
GM	USA	Chevy- Volt	Li-ion
		Saturn Vue Hybrid	NiMH
Ford	USA	Escape, Fusion, MKZ HEV	Ni-MH
		Escape PHEV	Li-ion
Toyata	Japan	Prius, LExus	NiMH
Honda	Japan	Civic, Insight	NimH
Hyundai	South Korea	Sonata	Lithium Polymer
Chrysler	USA	Chrysler 200C EV	Li-ion
BMW	Germany	ML450, S400	NiMH
		Mini E (2012)	Li-ion
BYD	China	E6	Li-ion
Daimler Benz	Germany	ML450, S400	NiMH
		Smart EV (2010)	Li-ion
Mitsubishi	Japan	iMiEV (2010)	Li-ion
Nissan	Japan	Altima	Ni-MH
		Leaf EV (2010)	Li-ion
Tesla	USA	Roadster (2009)	Li-ion
Think	Norway	Think EV	Li-ion, Sodium or Metal Chloride

2.1.3 Battery Characteristics

The key parameters that need to be considered while modeling EV batteries are described below.

2.1.3.1 Battery Capacity

Battery capacity is the maximum amount of energy that can be extracted from battery under specific conditions. It is determined by the mass of active material available in the battery. The capacity of battery is affected due to ageing, charging and discharging rate of battery, and the ambient temperature. It is measured in terms of Watt-hour (Wh) or Ampere-hour (Ah). Ah is commonly used in battery system as battery voltage change with variation in charging or discharging cycle. Ah represents the number of hours a battery can supply current. This amount is equal to the discharge rate of battery voltage. If the capacity of battery is 10 Ah, it can supply 10A current for 1 hour or 5A current for 2 hours. Wh is the product of Ah and nominal voltage of battery.

2.1.3.2 State of Charge

State of charge (SOC) is defined as available capacity of battery expressed as percentage of its rated capacity. For EVs, SOC is equivalent to fuel gauge. Mathematically, SOC can be expressed as,

$$SOC = \frac{A}{Q} \tag{2.1}$$

where

A is the available battery capacity, and

Q is the rated battery capacity.

Depth of discharge (DOD) is another means of measuring battery capacity. It is opposite of SOC. If the battery is fully charged, SOC is 100% and DOD is 0% and if it is fully discharged, SOC is 0% and DOD is 100%.

SOC of EV battery decreases with movement of EV from one location to another.

2.1.3.3 Charging Efficiency

Charging efficiency is the rate by which the electricity from the grid is supplied to the battery in usable form. Most of the energy is used in restoring original chemical condition in cell. Some of the energy is lost during the charging process in the battery and the charger as heat. The charging efficiency varies with the type of the battery charger and battery manufacturer. Charging process cannot be 100% efficient.

2.1.4 EV Charging Scheme

SOC of EV batteries decrease when EVs travel from one location to another. Hence, EVs are plugged in to the grid to charge their batteries. Different charging techniques can be implemented which are listed below:

2.1.4.1 Uncoordinated Charging Scheme

This is the most conventional charging scheme in which EVs are charged as soon as they arrive at any charging station, i.e., home or office. EVs owners' do not receive any incentive to use this technique. They do not have any information to schedule the charging time. When EVs are plugged in to distribution network and charged using this technique, most of EVs are charged during the time with peak system load. This will affect the voltage profile of the various nodes of distribution system.

2.1.4.2 Coordinated Charging Scheme

This is the similar to the uncoordinated charging technique, but when EVs are connected to the electricity network, charging process is controlled by smart grid aggregator based on time frame [23]. Charging process is delayed by certain time to avoid peak demand period. The delay time is based on information from the EV owner about their charging requirement and the time when the charging process has to be complete. The line loading are reduced by large amount as charging load are distributed over the large time frame. Sometime, while shifting loads, another peak are created which might negatively affect system voltage.

2.1.4.3 Smart Charging Scheme

In this technique, EVs are charged only when grid permits or requires to charge. Different optimization techniques are used to improve the operation of power network such as power factor, voltage profile improvement. An optimal EV charging schedule are obtained based on desired customer or grid objective. Communications are required between the grid operator and EV owner. Smart charging are also useful when renewable energy sources are integrated to the grid.

2.1.4.4 Vehicle to Grid Charging Scheme

This is the modified form of smart charging technique in which EVs can transfer power back to the grid. V2G service can be done by discharging energy through bidirectional power flow or through charge rate modulation with unidirectional power flow [24].

2.2 Distribution System

Power system consists of generating units, transmission system, and distribution system. Distribution system supplies electrical energy from transmission substations to different customers by converting voltage to suitable level. The customers may be residential, commercial, or industrial customers. Figure 2.3 shows the schematic diagram of power system.

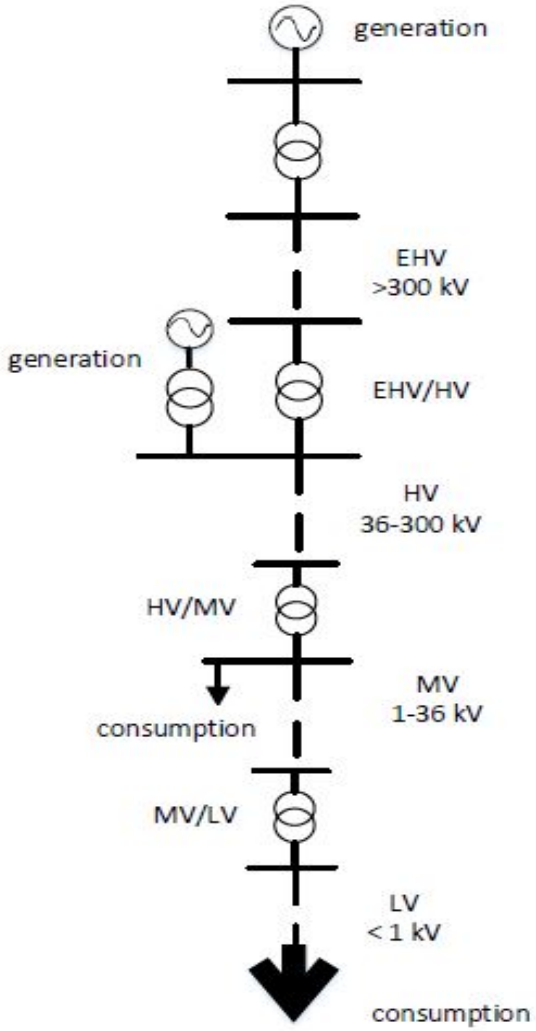

Figure 2.3. Schematic of transmission and distribution system [25]

Distribution system includes bulk power substations, sub-transmission lines,

distribution substations, primary feeder, distribution transformer, secondary circuit and service drops. Figure 2.4 shows the schematic diagram of radial distribution system. The function of each unit in distribution system is described below:

1) Bulk power substation

   Bulk power substation receives power from generating units through transmission lines and converts extra high voltage into sub-transmission voltage.

2) Sub-transmission system

   Sub-transmission system consists of circuits nominally rated at 69 kV. They are obtained from bulk power substation.

3) Distribution substation

   Distribution substation converts circuit from sub transmission system into primary feeder voltage.

4) Primary distribution circuits

   Primary distribution circuits are circuits from distribution substation and are responsible for supplying power for residential, commercial and industrial customers.

5) Distribution transformers

   Distribution transformers step down voltage from primary feeder to customer level voltage.

6) Secondary circuits and service drops

   They distribute electricity to customer premises from distribution transformer.

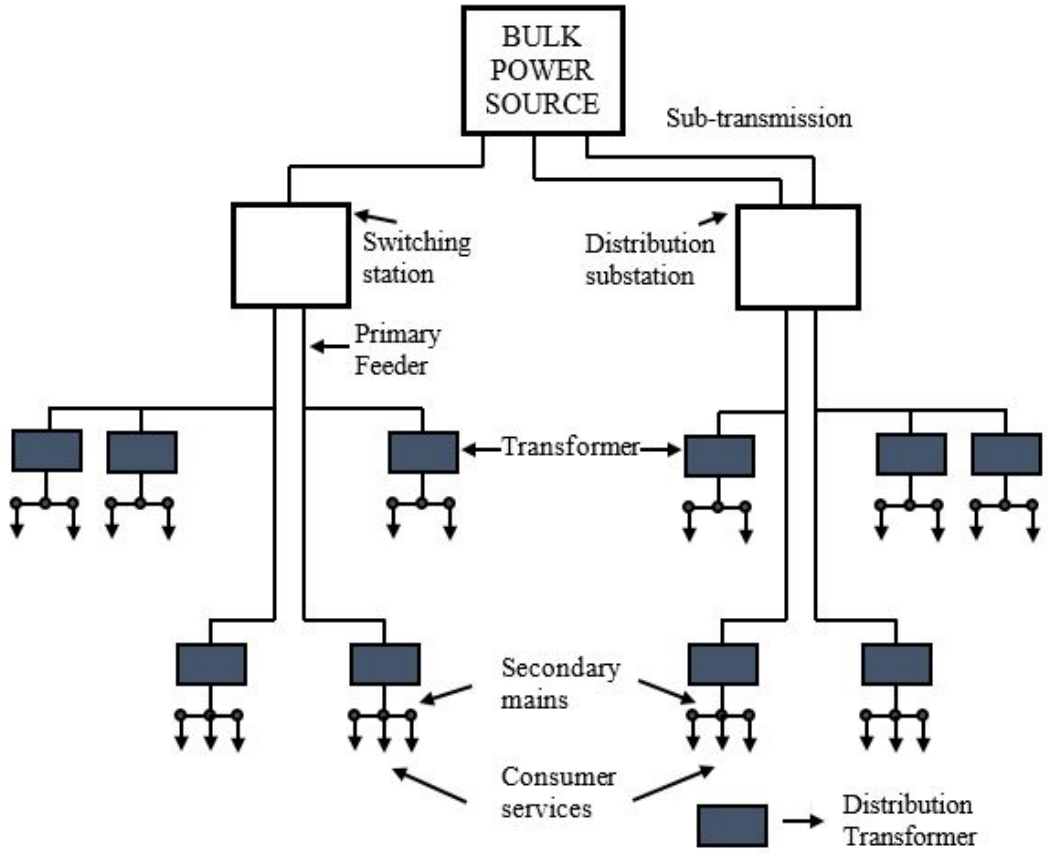

Figure 2.4. Distribution System [26]

Table 2.2 shows the typical voltage level that are used in various units of power network.

Table 2.2. Typical Voltage in Use [26]

Type	**Main Transmission**	**Sub Transmission**	**Primary Distribution**	**Distribution Secondary**
I	69,000 V	13,800 V	2,400 V	120 V
II	138,000 V	23,000 V	4,160 V	120/240 V
III	220,000 V	34,500 V	13,800 V	240 V
IV	345,000 V	69,000 V	23,000 V	277/480 V
V	500,000 V	138,000 V	34,500 V	480 V

2.2.1 Roy Billinton Test System

RBTS is a standard six bus system that is modeled for the purpose of reliability studies at the transmission level. It consists of two generator buses (Bus 1 and Bus 2) and five load buses (Bus 2- Bus 6). It has eleven generators and nine transmission lines. The total installed capacity of this system is 240 MW with peak load of 185 MW. It has four voltage levels i.e., 230 kV, 138 kV, 33 kV and 11 kV [27]. Figure 2.5 shows complete single line diagram of RBTS. Each bus can be used for purpose of modeling and simulation of distribution network.

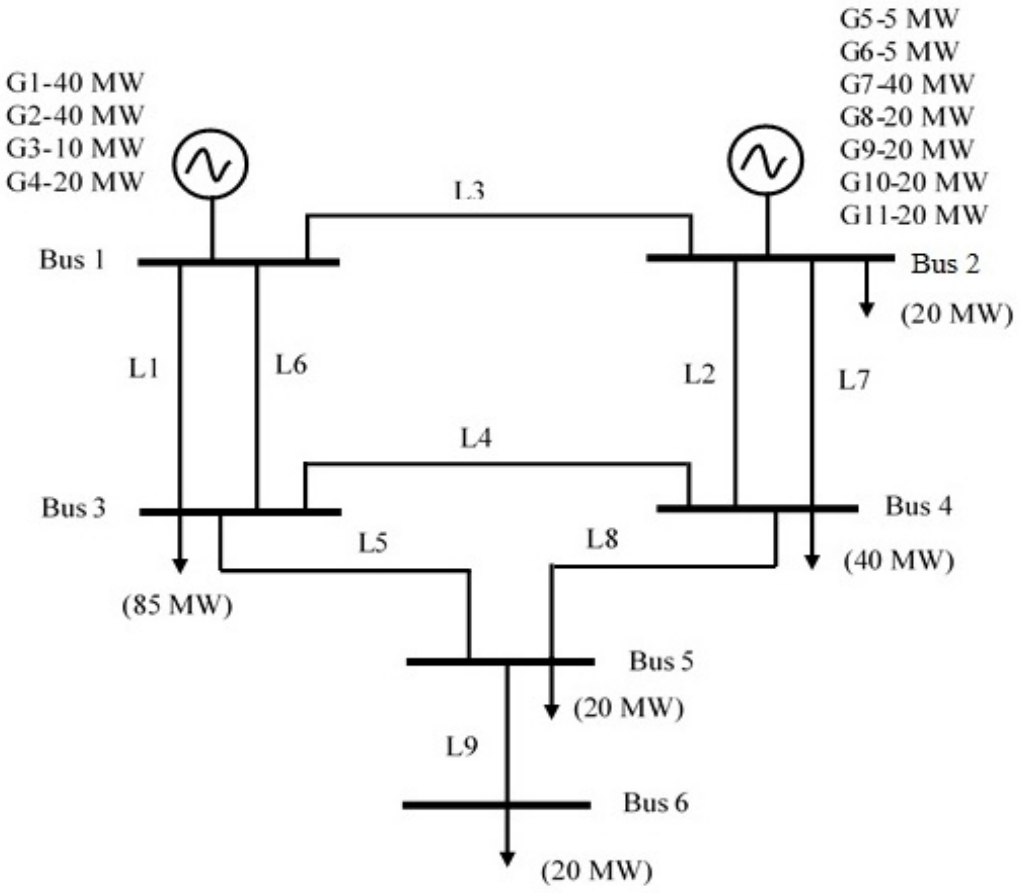

Figure 2.5. Single Line Diagram of RBTS [27]

2.2.1.1 RBTS Bus 5 Distribution System

RBTS Bus 5 distribution system represents typical urban areas with residential, commercial, office, and buildings and governmental customers. It consists of four feeders and twenty six load points. Among twenty six load points, thirteen load points are connected to residential customers, three load points to office buildings, five load points to the government and institutions, and remaining five to the commercial customers. The peak load of this system is 20 MW. Figure 2.6 shows the distribution network of RBTS Bus 5 system. Table 2.3 shows the classification of various load points based on customer type and their peak load.

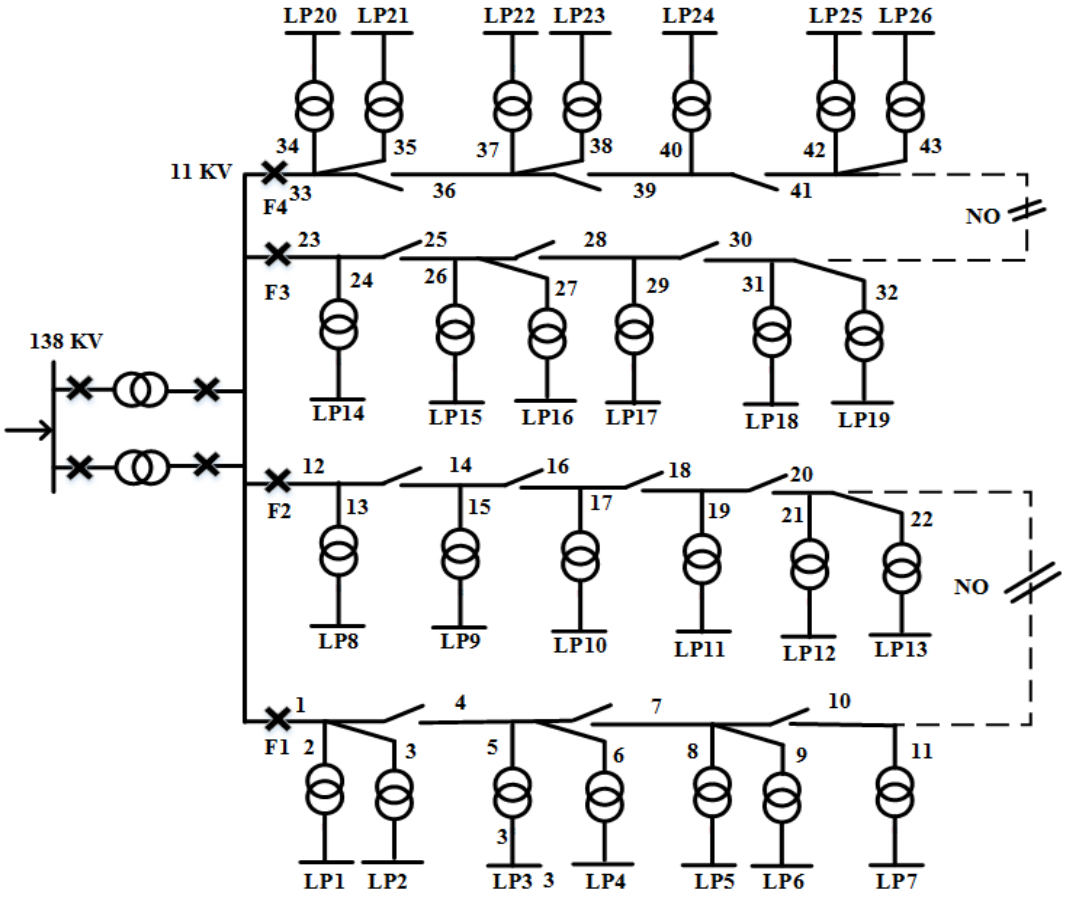

Figure 2.6. Distribution System for RBTS Bus 5 [27]

Table 2.3. Customer Data [27]

Number of loadpoints	**Loadpoints**	**Customer type**	**Peak load per loadpoint (MW)**
4	1, 2, 20, 21	Residential	0.76
4	4, 6, 15, 25	Residential	0.75
5	1, 26, 9, 10, 11, 13	Residential	0.57
5	3, 5, 8, 17, 23	Government	1.11
5	7, 14, 18, 22, 24	Commercial	0.74
4	12, 16, 19	Office building	0.62

2.3 Graph Theory

Graph theory is a branch of mathematics that deals with points and lines. Graph represents any network and their connection with each other. In graph, there are collection of vertices which are connected together by edges. Mathematically, a graph G is defined as an ordered pair with set of vertices V(G) connected by set of edges E(G) with incidence function ψ_G as,

$$G = \{V(G), E(G), \psi_G\} \tag{2.2}$$

Figure 2.7 represents a simple graph. The set of V(G), E(G) and ψ_G are expressed as,

$$V(G) = \{v_1, v_2, v_3, v_4, v_5\} \tag{2.3}$$

$$E(G) = \{e_1, e_2, e_3, e_4, e_5, e_6\} \tag{2.4}$$

$$\psi_G(e_1) = \{v_2, v_1\},\ \psi_G(e_2) = \{v_3, v_2\},\ \psi_G(e_3) = \{v_3, v_1\},\ \psi_G(e_4) = \{v_4, v_3\},\ \psi_G(e_5) = \{v_5, v_3\} \tag{2.5}$$

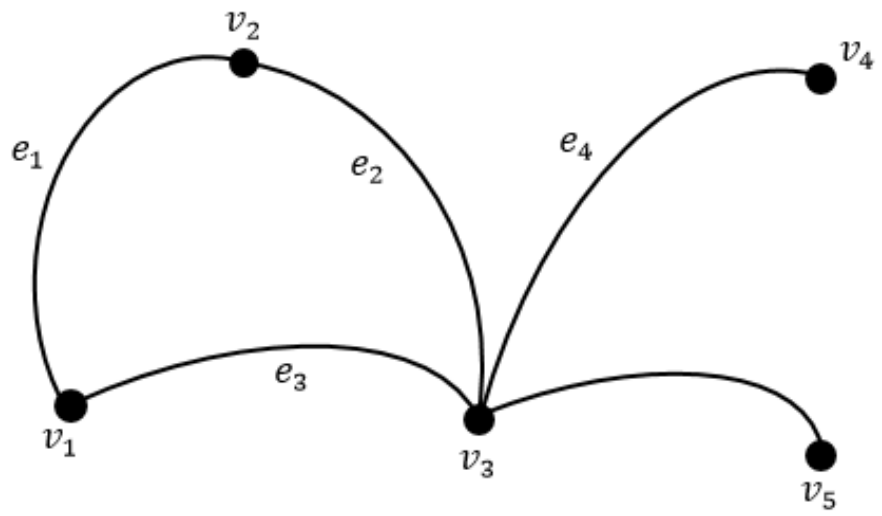

Figure 2.7. A Simple Graph [27]

Arrow sign represents the direction of edges. If arrow is not used, the path between two vertices is bidirectional. Graph theory are useful for representing complex networks. It can be used to model the road network, water supply network, power network, design of integrated circuits (ICs) for computers, etc. In road network, nodes represent crossroads/towns and edges represent distance between different streets. In power network, nodes represent different nodes of distribution network or buses of power system and edges represent distribution or transmission lines.

2.3.1 Dijkstra's Algorithm

Dijkstra's algorithm is used to determine the shortest path between a source node and other remaining nodes in the graph. The graph may be directed or undirected. In any graph, it is possible to have more than one shortest path between two vertices. Each path between two nodes are assigned with certain weight. The weight must be non-negative value for Dijkstra's algorithm. While determining shortest path between two nodes (i.e., traveling salesman), the shortest path may not travel through all vertices. The length of

shortest path between source node and destination node can be calculated. Consider a graph, G with source vertex, s such that $G = \{V, E, C\}$, $s \varepsilon E$ and $c_{ij} \geq 0$ for edge $(i, j) \varepsilon E$. c_{ij} is the cost of traveling path i to j. 'p' represents the permanent status for visited node and 't' represents temporary status for unvisited node. d_j represents distance of node j. The following steps are followed to determine the shortest path from s to remaining nodes.

1) Set zero distance value to node s since the cost to visit from node s to node s is zero and mark it as visited. The state of node s is $(0, p)$.

2) Assign cost to all other nodes as infinity and mark them as unvisited node. The state of other node is (∞, t).

3) Assign node s as current node.

4) Find set J of unvisited nodes that can be traveled from current node i by using path (i, j).

5) For each $j \varepsilon J$, the distance d_j is updated such that,

   new $d_j = \min\{d_j, d_i + c_{ij}\}$.

6) Find the node j with smallest distance among all nodes $j \varepsilon J$, then find $j*$ such that $\min_{j \varepsilon J} d_j = d_{j^*}$.

7) Set node j^* as visited/permanent node and mark this node as current node.

8) Repeat step (4) to (7) till all nodes are marked as permanent node.

9) Stop the process.

d_{j^*} represents the length of shortest path between source node s and other node j. The time complexity of Dijkstra's algorithm is the total time required to run this algorithm which is the function of total number of vertex V and number of edges E. The total run time is calculated as,

$$O(E\ logV) \tag{2.6}$$

Figure 2.8 shows an example of step wise working of Dijkstra's algorithm for determining shortest path between Node 1 and Node 6. Figure 2.8(a) represents a simple graph with six nodes represented with circle and paths represented with solid black lines. Number on the paths represent the distance (weights) between nodes. Let us assume an EV travels from Node 1 to Node 6. There are several possible paths EV may follow to travel from Node 1 to Node 6 such as 1-2-5-6 or 1-3-2-5-4-6 or 1-3-5-6 or 1-4-5-6. We are interested in finding shortest path. The graph is represented as,

$$V(G) = \{1,2,3,4,5,6\} \tag{2.7}$$

$$E(G) = \{e_1, e_2, e_3, e_4, e_5, e_6, e_7, e_8\} \tag{2.8}$$

$$\begin{aligned} &\psi_G(e_1) = \{v_2, v_1\} = 3, \psi_G(e_2) = \{v_3, v_2\} = 4, \psi_G(e_3) = \{v_3, v_1\} = 4, \\ &\psi_G(e_4) = \{v_1, v_4\} = 2, \psi_G(e_5) = \{v_2, v_5\} = 2, \psi_G(e_6) = \{v_3, v_5\} = 6, \\ &\psi_G(e_7) = \{v_6, v_4\} = 4, \psi_G(e_8) = \{v_5, v_4\} = 1, \psi_G(e_9) = \{v_6, v_5\} = 2 \end{aligned} \tag{2.9}$$

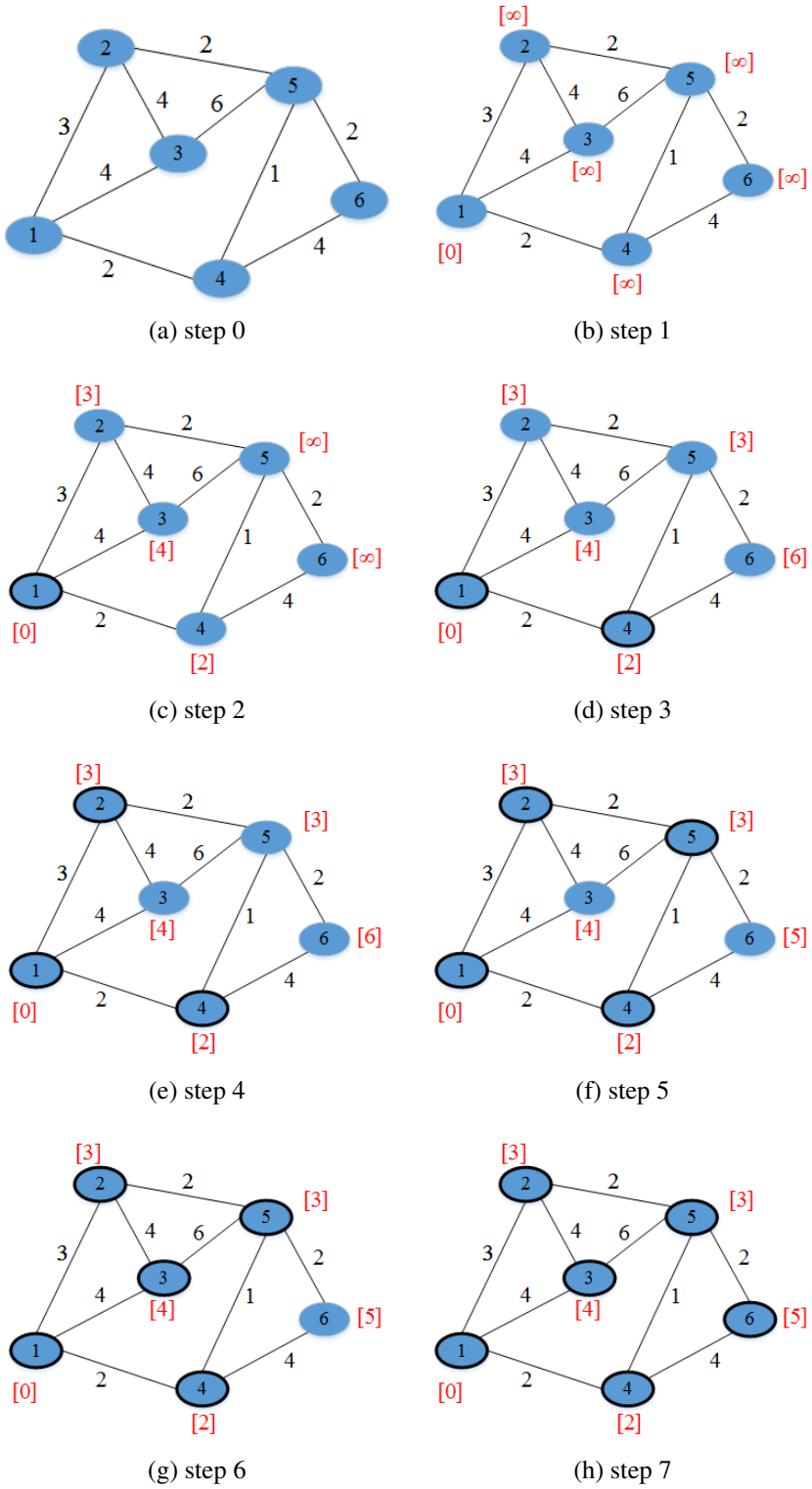

Figure 2.8. A simple graph with a Dijkstra's algorithm example

At first, Node 1 is selected as current node and its cost is assigned as zero.

Remaining nodes are marked as unvisited node and their weights are assigned as ∞ as shown in Figure 2.8(b). Then, the distance between Node 1 and its neighbouring nodes i.e., Node 2, Node 3 and Node 4 are calculated and their weights are updated as 3, 4 and 2 units respectively. Then, Node 1 is marked as visited node (represented by circle) and Node 4 is selected as current node in Figure 2.8(c). The distance of neighboring nodes of Node 4 i.e., Node 5 and Node 6 are calculated to be 3 unit and 6 unit respectively.Node 4 is marked as visited node which is shown in Figure 2.8(d). Since, both Node 2 and Node 5 have equal weight (3 unit), i.e., minimum weight among unvisited nodes, Node 2 is selected as current node. The new weight of Node 3 and Node 5 are calculated to be 7 and 5 respectively. Since, new weight of Node 3 and Node 5 are higher than previous weight, their weights remain unchanged. Node 2 is marked as visited node as shown in Figure 2.8(e). Node 5 is selected as current node. New value of neighboring nodes 3 and 6 are 9 unit and 5 unit respectively. Since the new value of Node 3 are higher, its value remains unchanged. Node 5 is marked as visited node and Node 3 is marked as current node as shown in Figure 2.8(f). Since all neighbouring nodes of Node 3 are visited, Node 3 is also marked as visited node as shown in Figure 2.8(g). Node 6 is marked as current node. Node 7 is also marked as visited node as all other nodes are visited as shown in Figure 2.8(h). So, the shortest path between Node 1 and Node 6 is 1-4-5-6 and the distance between them is 5 unit.

2.4 Load Flow Analysis

Load flow analysis is steady state analysis tool that calculates the voltage and angle magnitude at all buses. Information on real and reactive power demand, generator terminal

voltage, real power generation, and network topology are provided. It also determines the current injected to each node, the power injected to and from any bus, the line flow, and losses in the lines. It gives an overall view on how power flows in the system.

Load flow equations are non-linear equations which are represented by Equation 2.10 and 2.11.

$$P_k = \sum_{j=1}^{N} |V_k||V_j|(G_{kj}Cos(\theta_k - \theta_j) + B_{kj}Sin(\theta_k - \theta_j)) \tag{2.10}$$

$$Q_k = \sum_{j=1}^{N} |V_k||V_j|(G_{kj}Sin(\theta_k - \theta_j) - B_{kj}Cos(\theta_k - \theta_j)) \tag{2.11}$$

where

P_k is active power injected at node k.

Q_k is reactive power injected at node k.

V_k and V_j are voltages at node k and node j respectively.

θ_k and θ_j are phase angle at node k and node j respectively.

G_{kj} is conductance of line between node k and node j.

B_{kj} is susceptance of line between node k and node j.

AC power flow or DC power flow techniques are used to solve power flow equations. AC power flow technique can be Newton Raphson method or Gauss Seidel method. Out of four unknown variables in load flow equations, two are known and two are determined by solving Equation 2.10 and 2.11 at each bus type. In PQ bus, the active and reactive powers at each bus are known and voltage magnitude and phase angle are unknown. In PV bus, the active power and voltage magnitude are known and the reactive

power and voltage phase angle are unknown. In slack bus, the voltage magnitude and angle are known and active and reactive power are unknown. Voltage of slack bus is considered as reference bus.

Load flow analysis has great significance in the planning phase of any power system. It gives idea on whether the existing network can support the increasing load demand. Power system planners can decide whether they need to add more generators to meet power demand and prevent system from being overloaded. With proper design of power system, large control on initial investment and operating cost can be done.

2.5 National Household Travel Survey

National Household Travel Survey (NHTS) provides important information on how people use their vehicle [8]. The survey is conducted by American Federal Highway Administration from April 2008 to April 2009. More than 150 thousand households were randomly contacted using Computer Assisted Telephone Interviewing Technology. People were asked several questions regarding their driving behavior for a day. Each household member filled a travel survey form for the assigned date. They also provide trip information over 24 hour period. All information is focused on vehicle rather than person or household. Information regarding mode of transportation, length of route, time of travel, route for travel, reason for travel, etc. were collected. The survey involves all mode of transformation. NHTS are important to determine the position of vehicles at different time interval. They are also useful in determining navigation algorithm, designing charging station location of electric vehicles, and vehicle design.

2.6 Monte Carlo Simulation

Monte Carlo simulation is computerized mathematical technique that performs repeated random sampling to obtain statistical results. This technique runs simulations for hundreds or thousands of iteration choosing different randomly selected variables. The results describe the likelihood or probability of getting any result. The results obtained from simulation can be used to create probability distribution, confidence intervals, tolerance zones, and histograms. This method is useful when the model involves large number of random variables, the model is complicated, or non-linear. Better decisions can be taken to reduce the possible risks related with uncertainty. Monte Carlo simulations have wide range of applications in the field of engineering, applied statistics, computational biology, transportation, and the environment.

CHAPTER 3 PROCEDURE

The various procedures used to achieve the objective of this thesis are elaborated in this chapter. The following tasks were performed to accomplish the goal.[1]

Task 1: Develop benchmark model of integrated traffic and power network.

Task 2: Use Dijkstra's algorithm to find the shortest route between residential and commercial nodes.

Task 3: Modeling of EV users driving behavior.

Task 4: Design of state transition algorithm to find number of EVs at various nodes.

Task 5: Develop system model for the purpose of simulation.

Task 6: Use uncoordinated and semi-coordinated techniques for charging EV batteries.

Task 7: Perform load flow analysis and Monte Carlo simulation to analyze effect of EVs on distribution system.

3.1 Benchmark Model of Integrated Traffic and Power Network

An integrated traffic and power network incorporates both a road network and distribution system. To know the effect of EV penetration in the medium voltage distribution network, it is important to consider movement of EVs in traffic system. The capacity of EV batteries changes as they travel, and EVs need to be charged when they

[1]The part of this work related to modeling of integrated traffic and power network, state transition algorithm and uncoordinated charging technique has been accepted to publish in paper 'S. Shrestha and T.M. Hansen, "Spatial-Temporal Stochasticity of Electric Vehicles in Integrated Traffic and Power Network", 2016 IEEE International Conference on Electro/Information Technology, Grand forks, ND, May 19-21, 2016.' and work related to semi-coordinated charging technique, load flow analysis and Monte Carlo simulation has accepted to appear in paper 'S. Shrestha and T.M. Hansen, "Distribution Feeder Impacts of Electric Vehicles Charging in an Integrated Traffic and Power Network", North American Power Symposium 2016, Denver, CO, Sept 18-20, 2016.'

arrive at charging stations. The number of EVs at charging locations changes with time, impacting the EV charging load connected to the nodes. Therefore, an integrated traffic and power network similar to one proposed in [7] is developed, as shown in Figure 3.1, using graph theory. The benchmark model of the system was developed using 'gplot' command in MATLAB. The following command is used.

$$gplot(A, xy) \tag{3.1}$$

where

A is n-by-n adjacency matrix. $A(i, j)$ is zero if node i and j are not connected. $A(i, j)$ represents the distance between node i and node j if they are connected with each other.

n is the number of nodes in power network or number of crossroads in traffic network.

xy is an n-by-2 matrix with each element representing the Cartesian coordinates of location of nodes or crossroads.

In Figure 3.1, the length and width of traffic network are 15.28 km and 16.1 km, respectively. The grey color represents traffic system of city area and red color represents the distribution system network, i.e., RBTS Bus 5 distribution system. The grey dashed lines represent the streets and circles represent cross roads. Red lines represent the distribution lines with red triangles representing the nodes. To model the system, EVs are assumed to be in one of the following three states:

- State 1: EV is in a residential area;

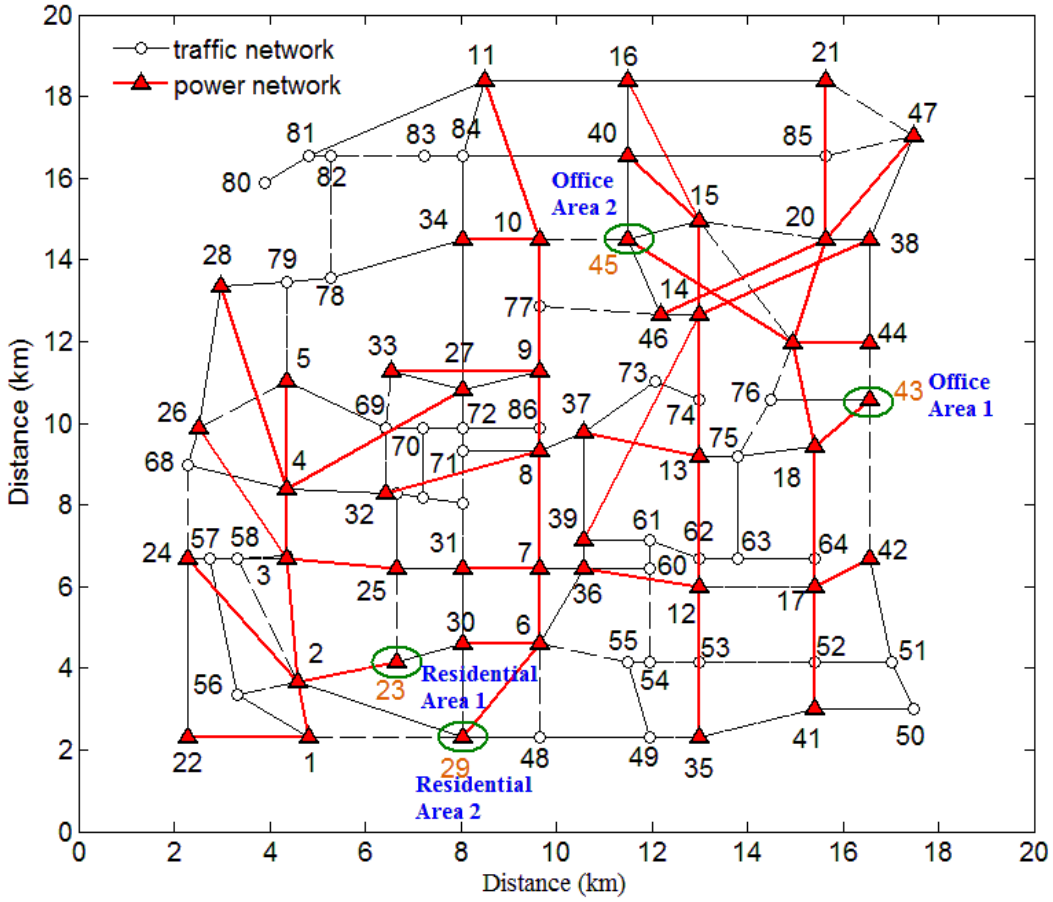

Figure 3.1. Integrated Traffic and Power System [7], [28]

- State 2: EV is in an office area; or
- State 3: EV is in transit.

In this work, two residential buses and two commercial nodes are considered for modeling the system. Node 23 and Node 29 are assumed as residential nodes that own EVs. Node 43 and Node 45 are assumed as commercial nodes, but the method is general enough to extend to *n* nodes. EVs travel from one residential bus to another commercial bus using traffic network. EVs are connected to the power network for charging their batteries when EV is in either State 1 or State 2.

3.2 Shortest Route between Residential and Commercial Node

There are several routes in traffic network which EV owners can use to reach their destination. In this work, for the purpose of modeling driving behavior, EV owners are assumed to follow shortest route to their destination. Residential nodes are assumed to be starting node and office nodes as destination node. EVs travel from each residential area to each office area. Each path is assigned with certain length, i.e., distance. Dijkstra's algorithm is used to determine the shortest path each EV uses. The MATLAB function 'dijkstra' was used to determine the shortest path and distance between these nodes. The usage of Dijkstra's algorithm is expressed by Equation 3.2.

$$[Cost,\ Route] = dijkstra(G,\ S,\ D) \tag{3.2}$$

where

S is the starting node,

D is the destination node,

G is an adjacency matrix that represent the value of the edge,

Cost is the shortest length between starting and destination node, and

Route is the shortest path an EV follows to reach destination node.

Table 3.1. Shortest Driving Distance

Location	**Residential Area 1**	**Residential Area 2**
Office Area 1	43.47 km	43.93 km
Office Area 2	39.56 km	40.48 km

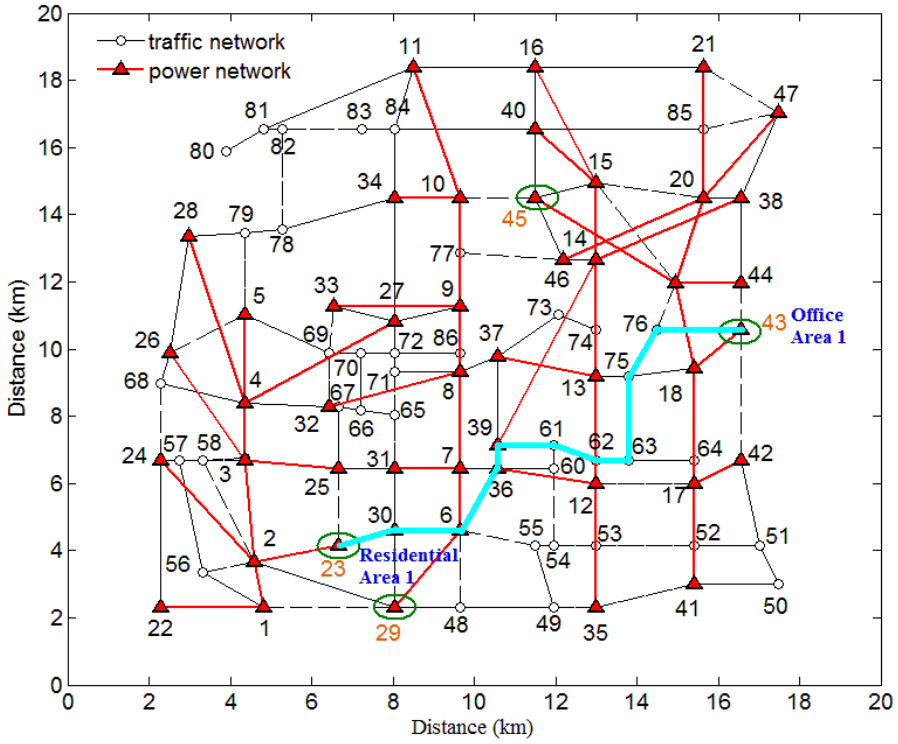

Figure 3.2. Shortest path between residential area 1 and office area 1

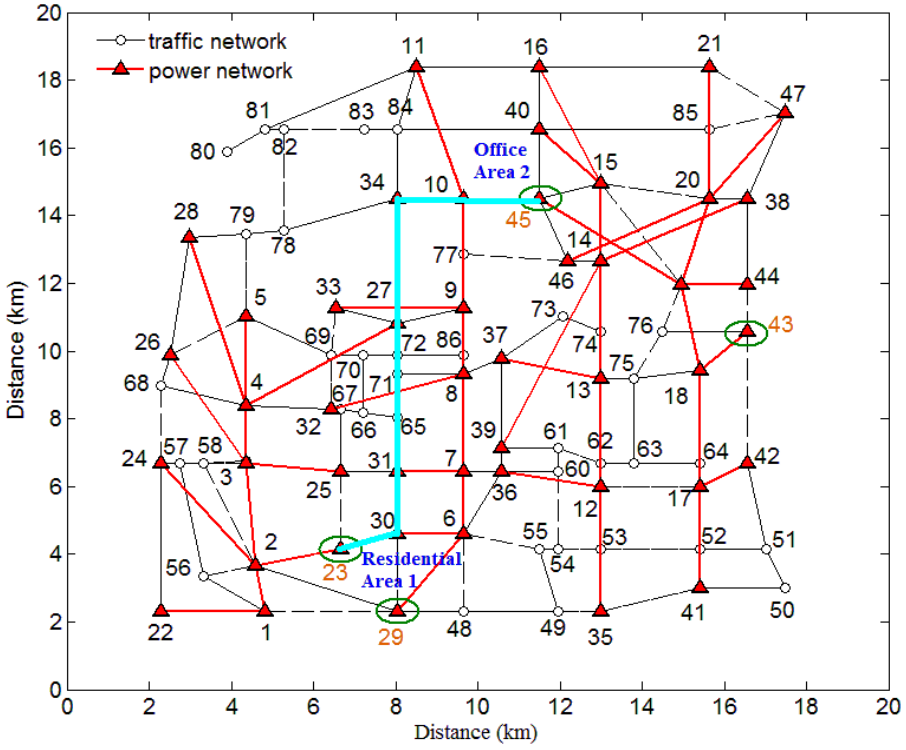

Figure 3.3. Shortest path between residential area 1 and office area 2

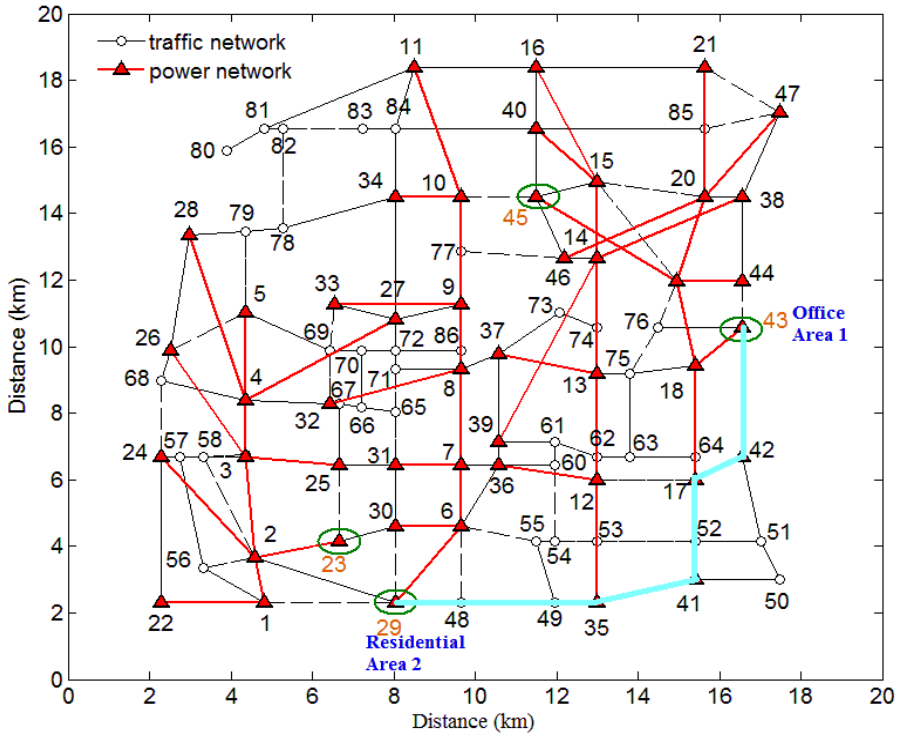

Figure 3.4. Shortest path between residential area 2 and office area 1

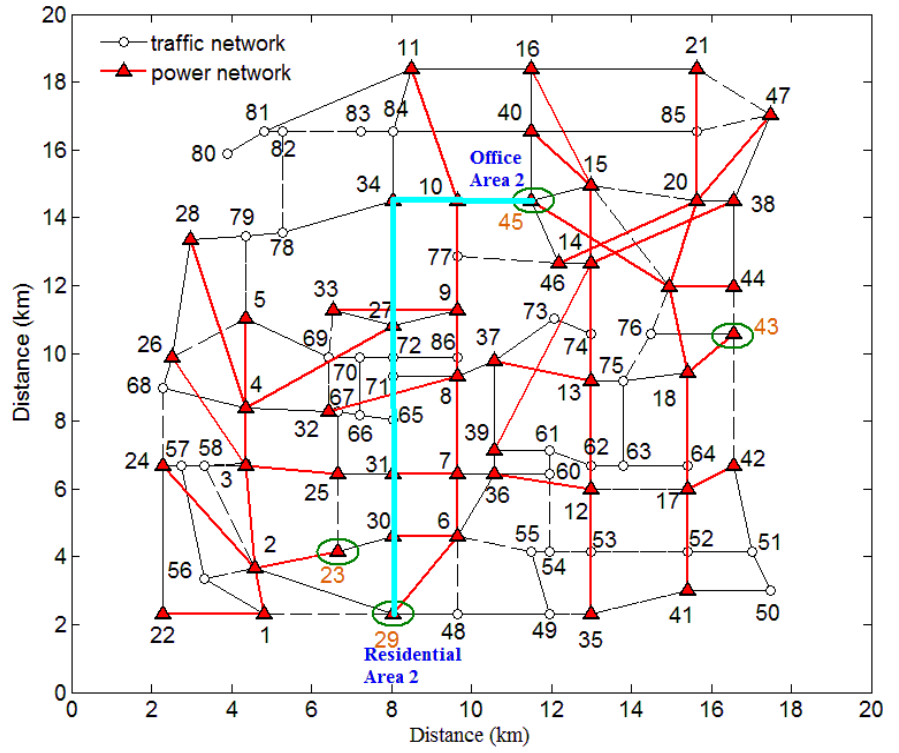

Figure 3.5. Shortest path between residential area 2 and office area 2

Solid lines (cyan color) in Figures 3.2, 3.3, 3.4, and 3.5 represent the shortest route between residential and office nodes. In this thesis, residential area 1 and residential area 2 connected to Nodes 23 and 29, respectively are starting nodes and office area 1 and office area 2 connected to Nodes 43 and 45, respectively are destination nodes or vice-versa. The shortest distance between these residential and office nodes are shown in Table 3.1.

3.3 EV Modeling

For modeling of EVs, information on departure time of EVs are taken from NHTS. Randomness in driving speed and parking duration are modeled using normal distribution. This method works for any EV battery, but in this work each EV is assumed to have Mitsubishi battery.

3.3.1 End User Driving Pattern

Figure 3.6 provides detail information of number of vehicles traveling from home to different destinations at different time interval in a day. The navy blue curve represents the total number of vehicles that move from home to office and vice-versa. In this work, the total number of vehicles represented by the navy blue curve in Figure 3.6 traveling before 10 am has been considered as the total number of vehicles moving from home to office, and the same number of vehicles travel back home after a certain time interval i.e., the rest period.

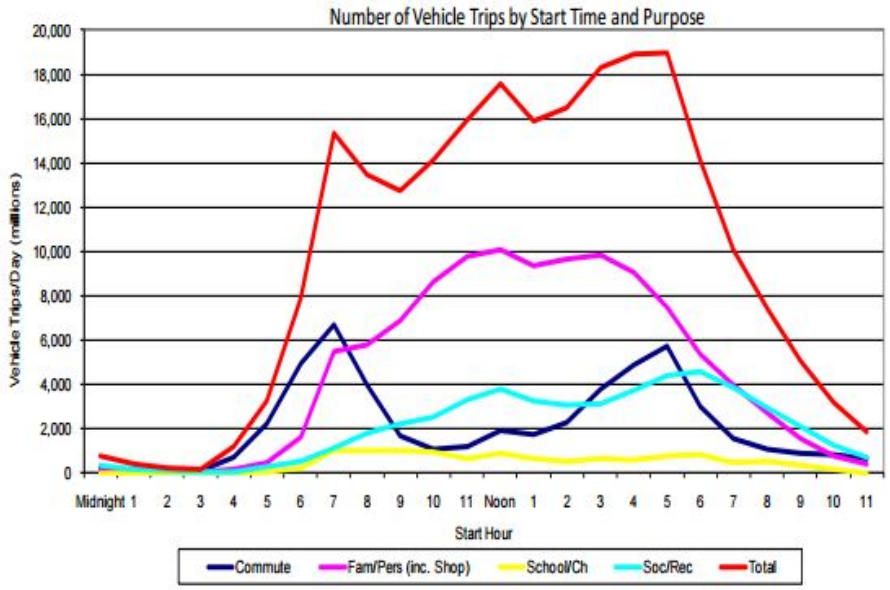

Figure 3.6. End User Driving Pattern [8]

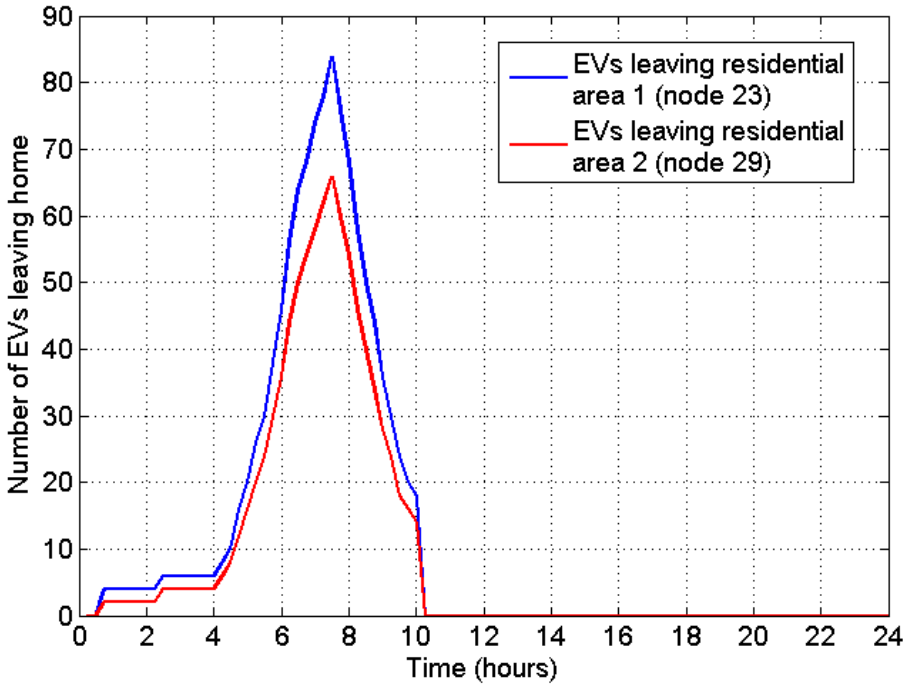

Figure 3.7. EVs leaving residential nodes [8]

Using Webplotdigitizer, discrete data were extracted from blue curve at 15 – minute time intervals. In this work, residential node 23 and 29 are assumed as point of common

coupling for 278 and 216 houses, respectively. Each household is assumed to have four EVs to highlight the negative impacts of EV charging. Hence, the number of vehicles are scaled down in such a way that total number of EVs connected to nodes 23 and 29 are 1,112 and 864, respectively. Out of total EVs, it is assumed that 50% of EVs travel to office area 1 and remaining 50% to office area 2. The distribution of EVs leaving these nodes based on their departure time at 15 – minute time interval for a day are shown in Figure 3.7.

3.3.2 End User Driving Speed

The speed of EVs vary according to drivers and routes taken. Most people in cities drive near the speed limit (the average speed), but some drivers' speeds lie above or below average speed. To make the driving behavior more realistic, the average speed (V_t) of EVs in a day are assumed to follow a normal distribution pattern $V_t \sim \mathrm{N}(\mu_t, \sigma_t)$ [29]. The probability density function of speed is

$$f(V_t, \mu_t, \sigma_t) = \frac{1}{2\pi\sigma_t^2} e^{-\frac{(V_t-\mu_t)^2}{2\sigma_t^2}} \tag{3.3}$$

where

V_t is the speed of EV at time 't',

μ_t is the mean of speed, and

σ_t is the standard deviation of speed.

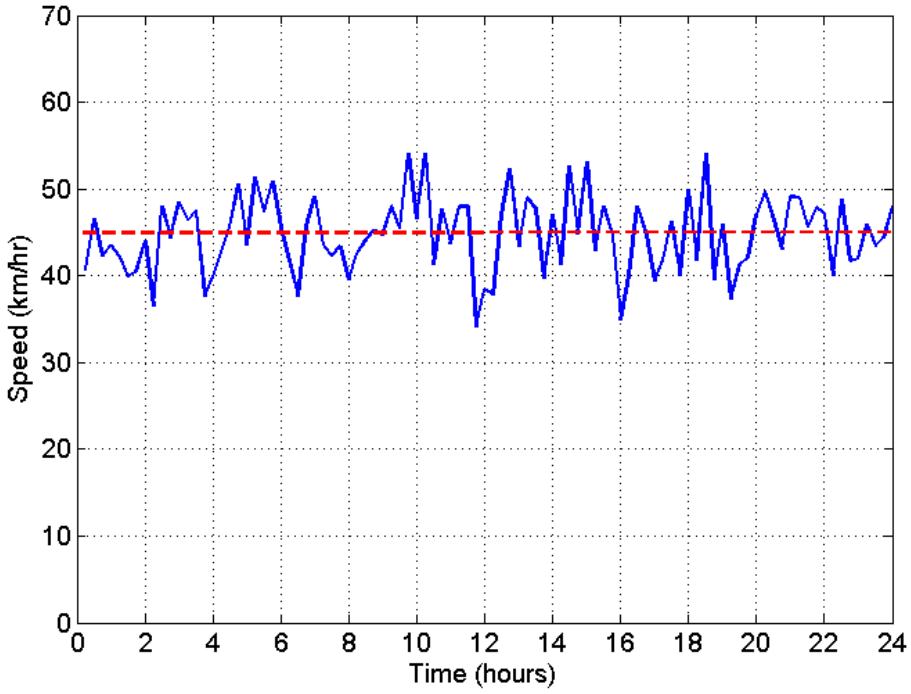

Figure 3.8. Speed of EVs leaving home at different time interval in a day

Here, the average speed of EVs are assumed to be 45 km/hr and standard deviation as 5 km/hr [30]. Figure 3.8 shows the speed of EVs leaving home at different time interval. Once V_t is known, time required to travel from home to office is calculated using Equation 3.4.

$$T_{ij} = \frac{d}{V_t} \tag{3.4}$$

where,

d is the shortest distance between bus i and bus j from Table 3.1.

3.3.3 Parking Duration

Parking duration varies according to driver. Due to uncertainty in driving behavior, some drivers may leave parking spot earlier or later than average parking duration. In this work, it is assumed that parking duration of EVs in any office follows a normal

distribution $T_{p,t} \sim \mathrm{N}(\mu_{p,t}, \sigma_{p,t})$ [7].The probability density function of parking duration is

$$f(T_{p,t}, \mu_{p,t}, \sigma_{p,t}) = \frac{1}{2\pi\sigma_{p,t}^2} e^{-\frac{(V_{p,t}-\mu_{p,t})^2}{2\sigma_{p,t}^2}} \tag{3.5}$$

where

$T_{p,t}$ is the parking time of EV that arrives at office at time 't',

$\mu_{p,t}$ is the mean of parking duration, and

$\sigma_{p,t}$ is the standard deviation of parking duration.

Here, average parking duration is assumed to be 7 hours and standard deviation is 1.75 hours [8]. Figure 3.9 shows the time EVs are parked at office when they arrive at office at different time interval.

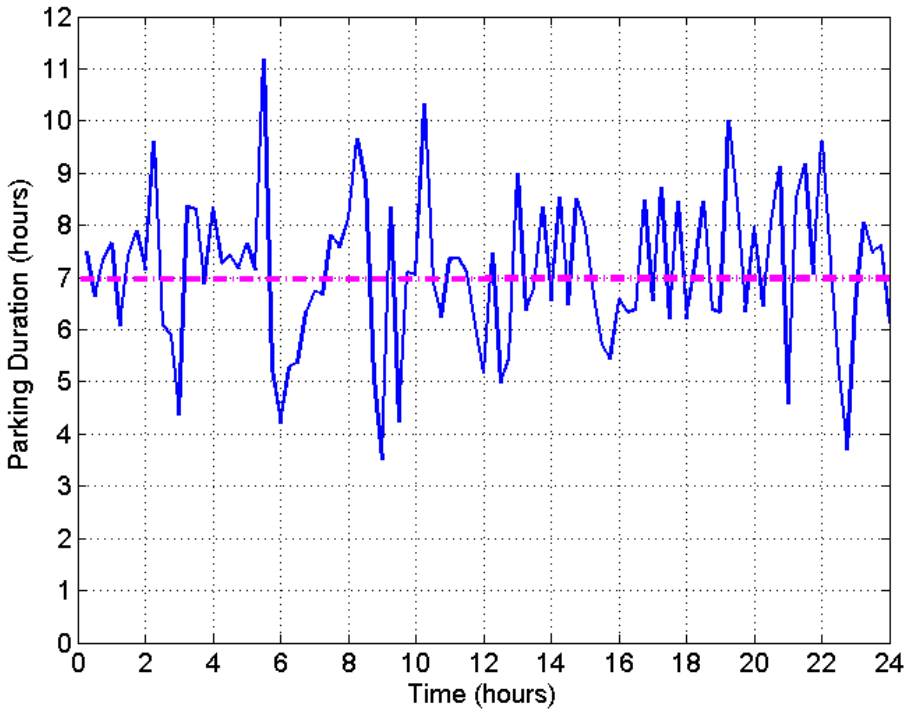

Figure 3.9. Parking duration for EVs arriving at office at different time interval in a day

3.3.4 Battery Model

Mitsubishi i-MiEV is one of the highly efficient car produced by Mitsubishi Motors. For the purpose of the simulation, it is assumed that all EVs contain same battery of type i.e., battery found in Mitsubishi i-MiEV. The capacity of each battery is 16 kWh [31]. Charging stations at office or home are assumed to have level 2 charger. These chargers charge battery at voltage level 220 V–240 V with the charging current of 15 A. According to SAE J1772 standard, the charging rate is 3.3 kW [31], [32]. It takes around 7 hours to fully charge the battery. So, the charging efficiency is considered as 90%. According to U.S. Environmental Protection Agency, the specific energy consumed by each battery is 0.1678 kWh/km [33].

3.3.5 State Transition Algorithm

A state transition algorithm is developed to calculate the number of EVs available at different home and offices at different time interval. Figure 3.10 shows a state switching model that shows movement of EVs from home area to office area.

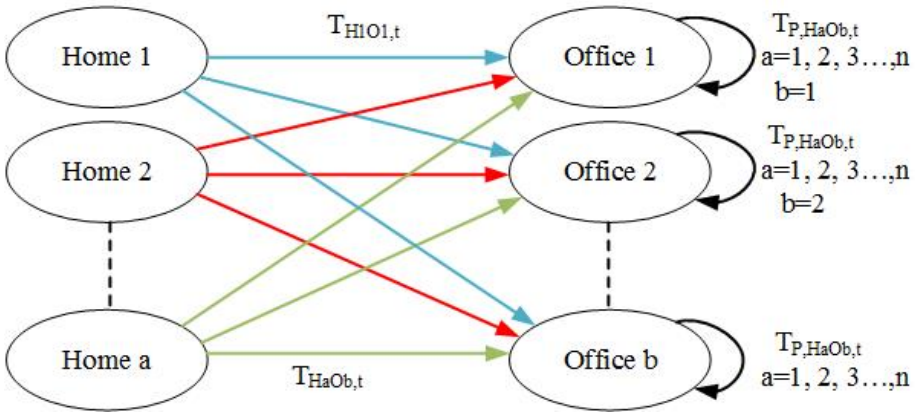

Figure 3.10. State Switching Model

Calculations are based on the assumption that

1) There is movement of EVs from each home to each office,

2) There is no movement of EVs between homes or between offices, and

3) All EVs start and end their journey at home.

Figure 3.11 represents simple working steps of state transition algorithm. Number of residential and commercial areas, EVs leaving home, nodes to which residential and commercial areas are located are given as input. From NHTS travel survey data, number of EVs leaving from home m to office n at 15 – minutes time interval, $n_{H_m O_n}(t)$, are obtained. The simulation is performed for 24 hours i.e. from 12 a.m. to 11:59 p.m. with 15 – minutes time interval. This algorithm is executed for $24 \times \frac{60}{15} = 96$ times.

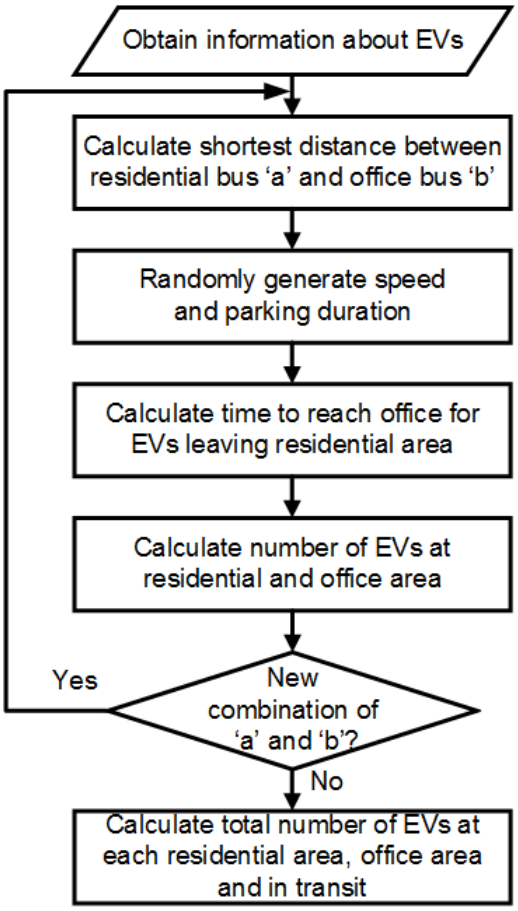

Figure 3.11. State Transition Algorithm

The various steps that are followed to calculate number of EVs at different time interval are explained in details below:

1) Input number of home (a) and offices (b); $m = 1,2,\ldots,a$ and $n = 1,2,\ldots,b$;

2) Input bus number to which home and offices are connected;

3) Initially $m = 1$ and $n = 1$;

4) Use Dijkstra's algorithm to calculate shortest path between each home and office, $(Y_{H_m O_n})$;

5) Randomly generate speed of EVs, $(V_{H_m O_n,t})$, traveling at different time interval using Equation 3.3;

6) Calculate time required to reach office from home or vice-versa;

$$T_{H_m O_n,t} = T_{O_n H_m,t} = \frac{Y_{H_m O_n}}{V_{H_m O_n,t}} \tag{3.6}$$

7) Calculate number of EVs that reach office at time 't';

$$n_{O_n}^{H^m}(t + T_{H_m O_n,t}) = n_{H_m O_n}(t) \tag{3.7}$$

8) Randomly generate parking duration at office; $T_{p,H_m O_n,t}$, using Equation 3.5;

9) Calculate number of EVs traveling from office to home at different time interval;

$$n_{O_n H_m}(t) = n_{O_n}^{H_m}(t + T_{p,H_m O_n,t}) \tag{3.8}$$

10) Calculate number of EVs that arrive home at time 't';

$$n_{H_m}^{O_n}(t + T_{O_nH_m,t}) = n_{O_nH_m}(t) \tag{3.9}$$

11) Calculate total number of EVs at home m due to movement of EVs from office n;

$$n_{H_m\text{-}O_n}(t+15) = n_{H_m\text{-}O_n}(t) + n_{H_m}^{O_n}(t+15) - n_{H_mO_n}(t+15) \tag{3.10}$$

12) Calculate total number of EVs at office n due to movement of EVs from home m;

$$n_{O_n\text{-}H_m}(t+15) = n_{O_n\text{-}H_m}(t) + n_{O_n}^{H_m}(t+15) - n_{O_nH_m}(t+15) \tag{3.11}$$

13) Repeat above steps from (3) to (12) for every combination of m and n;

14) Calculate total number of EVs at each home, office and in movement;

$$n_{H_m}(t) = \sum_{n=1}^{b} n_{H_m\text{-}O_n}(t) \quad where, m = 1,2...a \tag{3.12}$$

$$n_{O_n}(t) = \sum_{m=1}^{a} n_{H_m\text{-}O_n}(t) \quad where, n = 1,2...b \tag{3.13}$$

$$n_{H_{total}} = \sum_{n=1}^{b}\sum_{m=1}^{a} n_{H_m\text{-}O_n}(15) \tag{3.14}$$

$$n_{movement}(t) = n_{H_{total}} - \sum_{m=1}^{a} n_{H_m}(t) - \sum_{n=1}^{b} n_{O_n}(t) \tag{3.15}$$

15) Calculate probability of finding EVs at each home and office;

$$P_{H_m}(t) = \frac{n_{H_m}(t)}{n_{H_{total}}} \tag{3.16}$$

$$P_{O_n}(t) = \frac{n_{O_n}(t)}{n_{H_{total}}} \tag{3.17}$$

3.4 Charging Techniques

Uncoordinated and semi-coordinated charging methods are applied in this work.

3.4.1 Uncoordinated Charging Technique

EVs are connected to the grid for charging as soon as they are parked at any charging station, and the charging continues until the battery is fully charged or another trip begins. Here,

$$t_{charging} = t_{arrival} \tag{3.18}$$

where

$t_{charging}$ is the time at which EVs start charging, and

$t_{arrival}$ is the time at which EVs arrive at a charging station.

If an EV leaves home 'm' at time 't_1' and arrives at office 'n' at time 't_2', then SOC of each EV battery at time 't_2' is calculated using Equation (3.19).

$$SOC(t_2) = SOC(t_1) - \frac{uy}{e} \times 100 \tag{3.19}$$

where

e is total battery capacity of each EV,

y is distance between home m and office n in km, and

u is energy consumption in kWh/km.

If an EV stays parked at the office for time 't_p', then the SOC of the EV battery before the return trip is calculated using Equation (3.20).

$$SOC(t_2+t_p) = min(SOC(t_2) + \frac{\eta \times Q \times t_p \times 100}{e}, 100) \tag{3.20}$$

where

η is the charging efficiency, and

Q is the charging rate in kW.

If an EV reaches home 'm' at time 't_3' in the evening from the office, then SOC of EV battery at time 't_3' is calculated using Equation (3.21).

$$SOC(t_3) = SOC(t_2+t_p) - \frac{uy}{e} \times 100 \tag{3.21}$$

Once, the SOC is known, the available battery capacity at each charging station at each time intervals can be calculated. If the number of EVs arrive at office at time T_1, T_2,...,T, then, the capacity of batteries available at office at any time 't' are calculated using equation (3.22).

$$C_{office}(t) = SOC(T_1+t)\times e \times n_{O_n}^{H_m}(T_1) + SOC(T_2+t)\times e \times n_{O_n}^{H_m}(T_2) + ... + SOC(T)\times e \times n_{O_n}^{H_m}(t) \tag{3.22}$$

Here, $SOC(T_n + t)$ can be calculated as,

$$SOC(T_n + t) = min(SOC(T_n) + \frac{\eta \times Q \times (t - T_n) \times 100}{e}, 100) \tag{3.23}$$

$$SOC(T_n) = SOC(t_{l-n}) - \frac{uy}{e} \times 100 \tag{3.24}$$

where

T_n = T_1, T_2,...,T, and

t_{l-n} is the the time at which EVs that arrive at office at time T_n leave home.

If the number of EVs arrive at home at time t_1, t_2,..., t, then the capacity of batteries available at home at time 't' are calculated using Equation 3.25.

$$C_{home}(t) = SOC(t_1 + t) \times e \times n_{H_m}^{O_n}(t_1) + SOC(t_2 + t) \times e \times n_{H_m}^{O_n}(t_2) + ... + SOC(t) \times e \times n_{H_m}^{O_n}(t) \tag{3.25}$$

Here, $SOC(t_n + t)$ can be calculated as,

$$SOC(t_n + t) = min(SOC(t_n) + \frac{\eta \times Q \times (t - t_n) \times 100}{e}, 100) \tag{3.26}$$

$$SOC(t_n) = SOC(T_n + t_p) - \frac{uy}{e} \times 100 \tag{3.27}$$

where

t_n=t_1, t_2,...,t.

The uncharged battery capacity, $C_{uncharged}$, at time 't' can be calculated using

Equation 3.28.

$$C_{uncharged}(t) = C_{fullcharged}(t) - C_{avaiable}(t) \tag{3.28}$$

where

$C_{full\ charged}$ is the total capacity of batteries if all EVs are fully charged, and

$C_{available}$ is the available capacity of batteries.

3.4.2 Semi-Coordinated Charging Technique

In this method, once EVs arrive at any charging station, they are connected to gird for charging only after certain time delay. If EV arrives at any location at time 't_2' and is parked for time '$t_{parking}$', then time taken to charge EV ($t_{charging}$) are calculated by using Equation (3.29) or (3.30).

$$t_{charging} = \frac{(SOC(t_2 + t_p) - SOC(t_2))e}{\eta Q}, \quad if\ t_{charging} \leq t_{parking} \tag{3.29}$$

$$t_{charging} = t_{parking}, \quad otherwise \tag{3.30}$$

At home, the time at which EVs start charging is represented by a uniform distribution $t_{delay\_home} \sim \mathrm{U}(t_{arrival\_home}, t_{limit\_home})$.

$$t_{limit\_home} = 12am + 0.5 \times R - t_{charging\_home} \tag{3.31}$$

where

$t_{arrival\_home}$ is the time when EVs arrive at home,

R is the rank whose value is 1 for first group of EVs that arrive at home from office,

2 for second group of EVs and so on, and

$t_{charging\_home}$ is the total time required to fully charge EV batteries at home.

At office, the delay in charging time is represented by uniform distribution $t_{delay\_office} \sim \mathrm{U}(t_{arrival\_office}, t_{limit\_office})$.

$$t_{limit\_office} = t_{departure\_office} - t_{charging\_office} \tag{3.32}$$

$$t_{departure\_office} = t_{arrival\_office} - t_{parking\_office} \tag{3.33}$$

where

$t_{arrival\_office}$ is the time when EVs arrive at office,

$t_{departure\_office}$ is the time when EVs leave office, and

$t_{parking\_office}$ is the time for which EVs stay at office.

SOC of the batteries between the time interval when EVs arrive at any charging station and the charging begin is same as the SOC at the beginning when they arrive at that charging station. If EVs arrive at office at time 't_1' and then start charging at 't_d', then SOC of EVs at time 't' are calculated using Equation (3.34) and (3.35).

$$SOC(t_d + t) = min(SOC(t_d) + \frac{\eta \times Q \times (t - t_d) \times 100}{e}, 100) \tag{3.34}$$

$$SOC_{(}t_d) = SOC(t_1) \tag{3.35}$$

The available and uncharged batteries capacity are calculated in the similar way as in uncoordinated charging technique described in Section 3.4.1.

3.5 EV charging load

When EVs whose SOC is not 100% are charged, they act as additional load to the grid. EV charging load ($EV_{charging\_load}$) at any charging station are calculated using Equation 3.36.

$$EV_{charging\_load}(t) = Q \times N_{EVs}(t) \tag{3.36}$$

where

$N_{EVs}(t)$ is the total number of EVs at any charging station at time 't' whose SOC is not equal to 1, i.e., whose batteries are not fully charged.

If N_1, N_2,...,N EVs arrive at office 1 and start charging at time T_1, T_2,...,T, then total EV charging load, EV_{load}, at time 'T' is calculated using Equation 3.37.

$$EV_{load}(T) = N_1 \times F_1 \times Q + N_2 \times F_2 \times Q + \ \ldots \ + N \times F \times Q \tag{3.37}$$

where

F_i is the variable whose value is 1 if $SOC(T_i + T) < 1$ and 0 if $SOC(T_i + T) = 1$, i=1,2,..,n.

$SOC(T_i + T)$ is calculated using Equation 3.23 or 3.34.

3.6 System Load

System load are assumed to vary with respect to time in a day in residential and commercial nodes with EVs. Hence, different load profile are considered for the residential and commercial customers with EVs. Figure 3.12 shows the daily load curve of residential area 1(magenta curve), residential area 2 (blue curve), office area 1 (red

curve), and office area 2 (green curve) The peak load of residential area 1, residential area 2, office area 1 and office area 2 are 0.76 MW, 0.59 MW, 0.74 MW and 0.74 MW, respectively [34]. Residential areas have peak load from 4 pm to 6 pm while office areas have peak load from 10 am to 4 pm. It is because most of the loads are consumed by lighting units and electric heaters during evening time at home. Electricity is consumed mainly by computers and printers during daytime at office. The same load curve is considered for office area 1 and office area 2, hence the red and green curve are overlapped in Figure 3.12. Loads on remaining nodes in RBTS Bus 5 system are assumed to be constant. The peak loads at various nodes of RBTS bus 5 are explained in Section 2.2.1.1. In load flow analysis, these loads represent the load demand at various nodes of distribution power system.

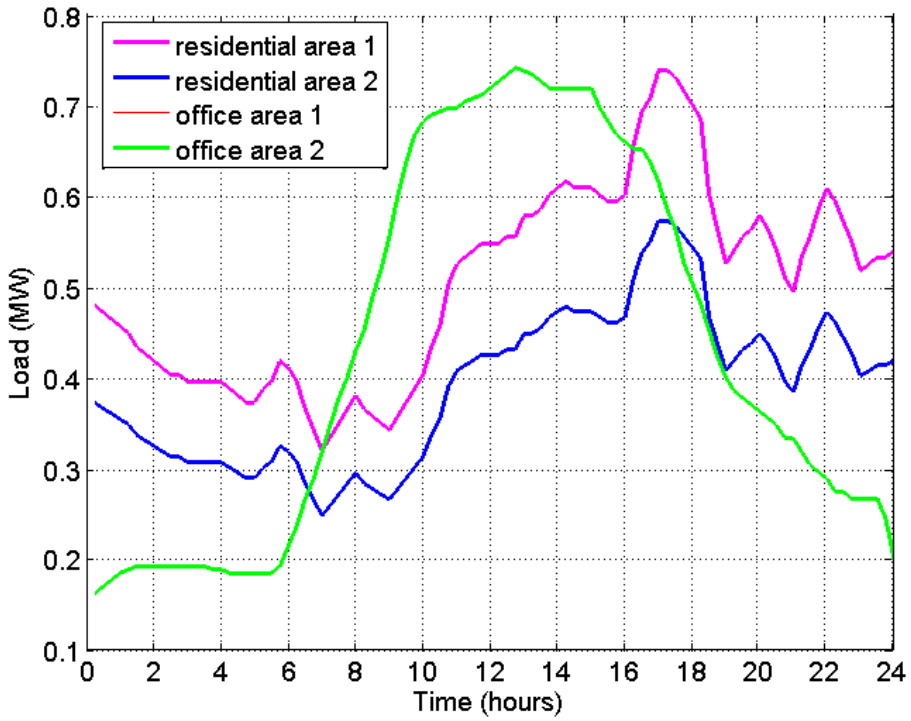

Figure 3.12. System Load for residential areas (magenta and blue curves) and commercial areas (red and green curves). The two office areas are assumed to have the same load profile, hence the curves overlap. [34]

3.7 Calculation of nodal voltage using load flow analysis

MATPOWER is used as simulation tool for performing load flow analysis [35]. EV charging loads are connected to the various nodes of distribution system, increasing the total demand. The total demand of the system (L_{total}) is calculated using Equation 3.38.

$$L_{total} = L_{system} + EV_{load} \tag{3.38}$$

where

L_{system} is the system load, and

EV_{load} is the total EV charging load.

To observe the impact of these loads on voltage profile of RBTS Bus 5 distribution system, load flow analysis is performed for a single day. The permissible node voltage in medium voltage distribution networks is assumed to be 0.95 to 1.05 p.u. Newton-Raphson method is used to determine the voltage profile at each node for each case. Each of the line impedances for the three phases are assumed to be the same. In this work, a balanced three-phase approximation is used. The line impedance of single phase lines of RBTS Bus 5 distribution system are shown in Table 3.2.

Table 3.2. Line Impedance of RBTS Bus 5 Distribution System

Type	**Impedance (Ω)**
Main Feeder	0.211 + 0.414j
Lateral Feeder	0.341 + 0.456j

The rating of the transformer in main feeder is 15 kVA and in lateral feeder is 8.8 kVA. The distribution system for Bus 5 has two 138/11 kV transformers. Each feeder has

voltage level of 11 kV. Each load points are supplied by 11/0.415 kV transformer. Only active loads are considered in this work.

3.8 Calculation of average nodal voltage using Monte Carlo simulation

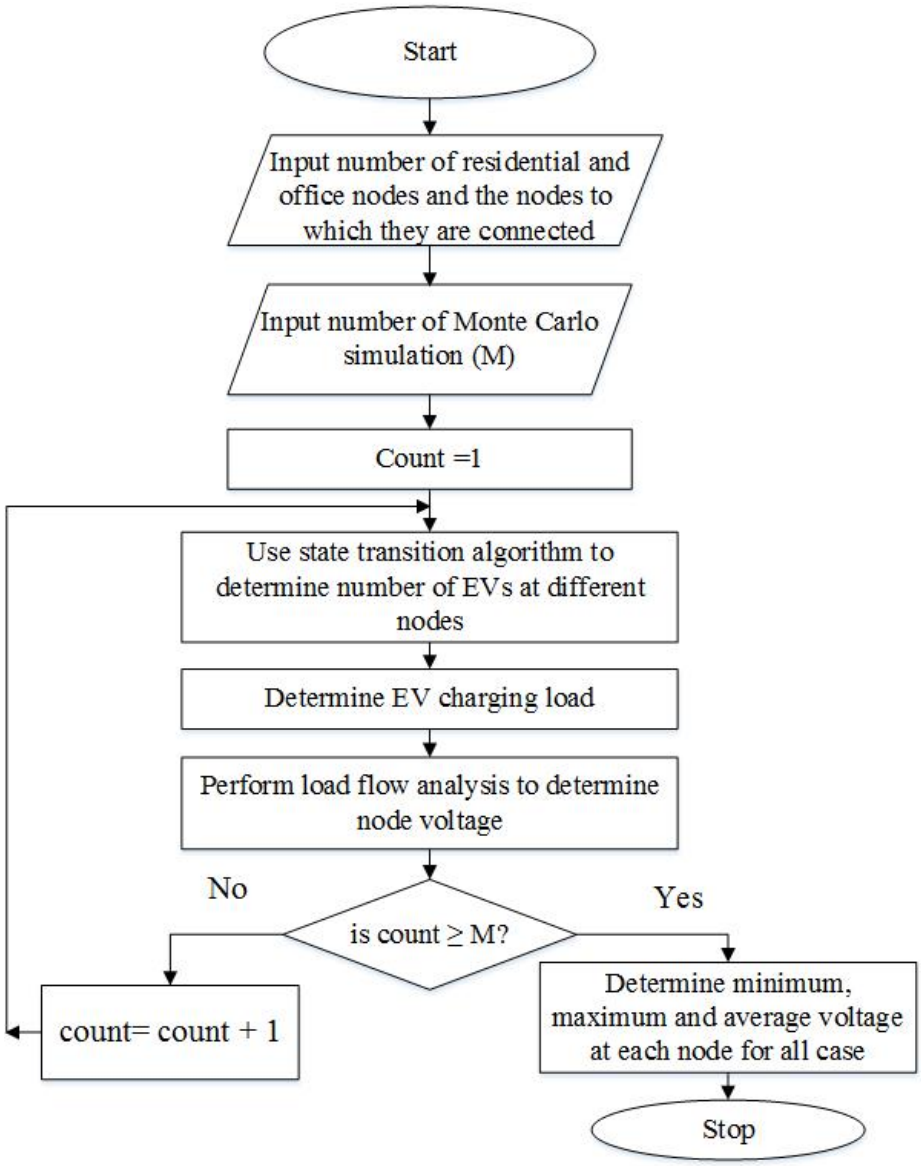

Figure 3.13. Flowchart for Monte Carlo simulations for determining voltage at each node based on the movement and charging of EVs.

Each time the program is executed, the total number of EVs available at any home or office at any time interval are found to be different due to the randomness in the driving

speed and parking duration. This will cause variations in EV charging loads and the voltage profile of the system. Therefore, the simulation is run 50 times, and the range of the minimum and maximum voltage at each node at different time intervals is determined. The average value of the voltage is calculated to observe whether or not the voltage at each node lies within permissible limits. The minimum voltage at each node at any time interval is the voltage that is found to be lowest at that node among the values obtained over 50 simulations. The average voltage at each node at any time interval is the value calculated by taking mean of all the voltages obtained over 50 simulations. Figure 3.13 shows flowchart for calculating minimum and average voltage using Monte Carlo simulations.

3.9 Simulation Cases

Four cases were considered for the purpose of simulation and analysis. These cases were used to calculate EV charging loads for different charging scenarios and analyze their impacts on node voltages. In case 1 and case 3, EVs were charged at home only using uncontrolled and semi-coordinated charging technique, respectively. EV charging loads were shifted at office during afternoon to reduce peak loads at home during the evening. Hence, in case 2 and case 4, EVs were charged both at home and office using uncoordinated and semi-coordinated charging technique, respectively. Table 3.3 contains the summary of all four cases.

Table 3.3. Simulation Cases

Case	**Description**
Case 1	EVs are charged only at home using uncoordinated charging technique
Case 2	EVs are charged both at home and office using uncoordinated charging technique
Case 3	EVs are charged only at home using semi-coordinated charging technique
Case 4	EVs are charged both at home and office using semi-coordinated charging technique

CHAPTER 4 RESULT AND ANALYSIS

Chapter 4 shows results and analysis obtained from simulation of EV model developed in integrated traffic and power system. Results for residential node 23 and commercial node 43 are only presented. The distribution of EVs with respect to time and space are presented. EV charging load are shown for different cases. The voltage profile at various nodes due to this EV charging loads are demonstrated. Finally, average voltage obtained from Monte Carlo simulations are also presented.

4.1 Location of EVs in Integrated Traffic and Power Network

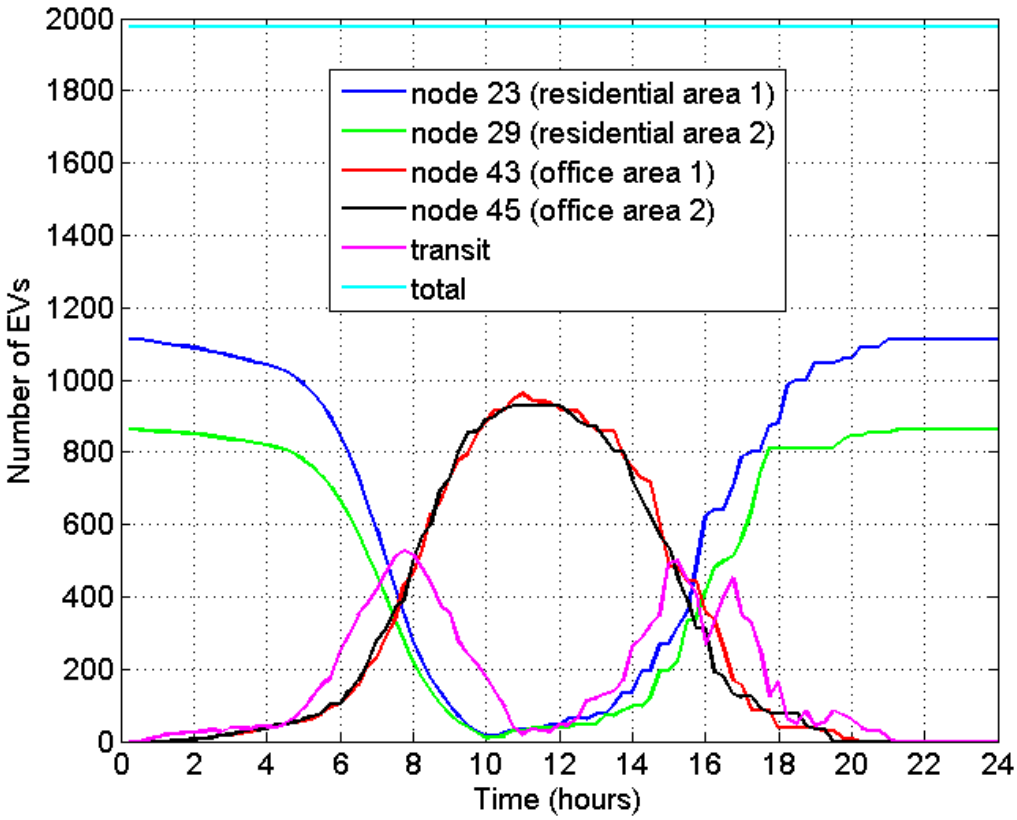

Figure 4.1. Number of EVs available at different locations in a day

Figure 4.1 shows the number of EVs available at different locations (i.e., at residential area, office area, or in transit) at different time intervals in the simulated day. It can be observed that the number of EVs is higher in residential areas (represented by the green and blue curve in Figure 4.1) during the morning and evening. The number of EVs is high at residential areas from 12 am until 7 am, and starts to decrease during the daytime. From 9 am until 3 pm, most EVs are parked in office areas (represented by the red and black curves in Figure 4.1). During the evening after 6 pm, the number of EVs increases in residential areas because EVs start to return home from the office. The number of EVs in transit, represented by the magenta curve in Figure 4.1, has two peaks, i.e., from 7 am to 9 am and 3 pm to 5 pm. This is due to movement of EVs from home to the office in the morning and the movement of EVs from the office back home in the evening. The zigzag pattern in these curves is due to the randomness in driving speed and parking duration. The total number of EVs, represented by cyan curve, at each time interval is constant.

Figure 4.2 shows the total probability of finding EVs at different locations. It follows a pattern similar to Figure 4.1, as the probability of finding EVs at any location is directly related to the number of EVs at that location. The probability is calculated based on the total number of EVs taken for simulation. The probability of finding EVs is higher in the morning and evening in residential areas, and office areas in the afternoon.

4.2 Capacity of EV batteries available at different location

Because the SOC of EV batteries decrease due to the movement from one location to another, EV batteries are charged when they are parked. EVs are connected to the

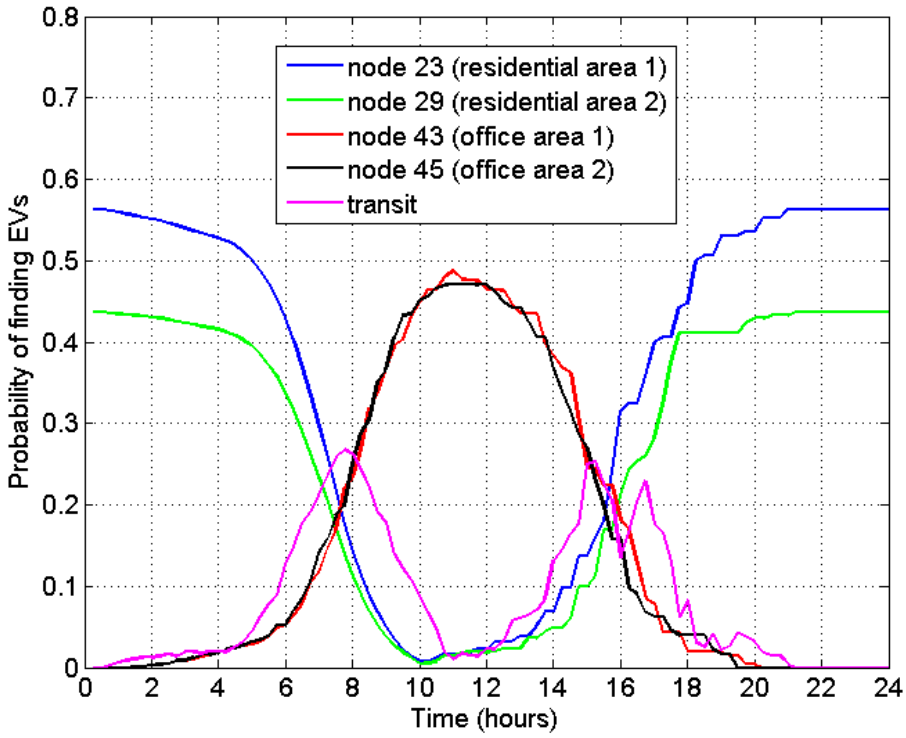

Figure 4.2. Probability of finding EVs at different locations in a day

power network through charging stations as soon as they arrive at a charging location or after certain time delay, and are until they are fully charged or next trip starts. Four different charging scenarios explained in Section 3.9 are analyzed.

4.2.1 Capacity of EV batteries at residential nodes when no charging occurs at office

Figure 4.3 shows the capacity of EV batteries available at residential node 23 when EVs are charged only at home. Solid lines represent the cases when EVs are charged using uncoordinated charging technique (Case 1). Dashed lines represent the cases when EVs are charged using semi-coordinated charging technique (Case 3). Capacity of batteries available for charging at any time, i.e., uncharged battery capacity is represented by blue curve. Capacity of batteries available at Node 23 is represented by red curve

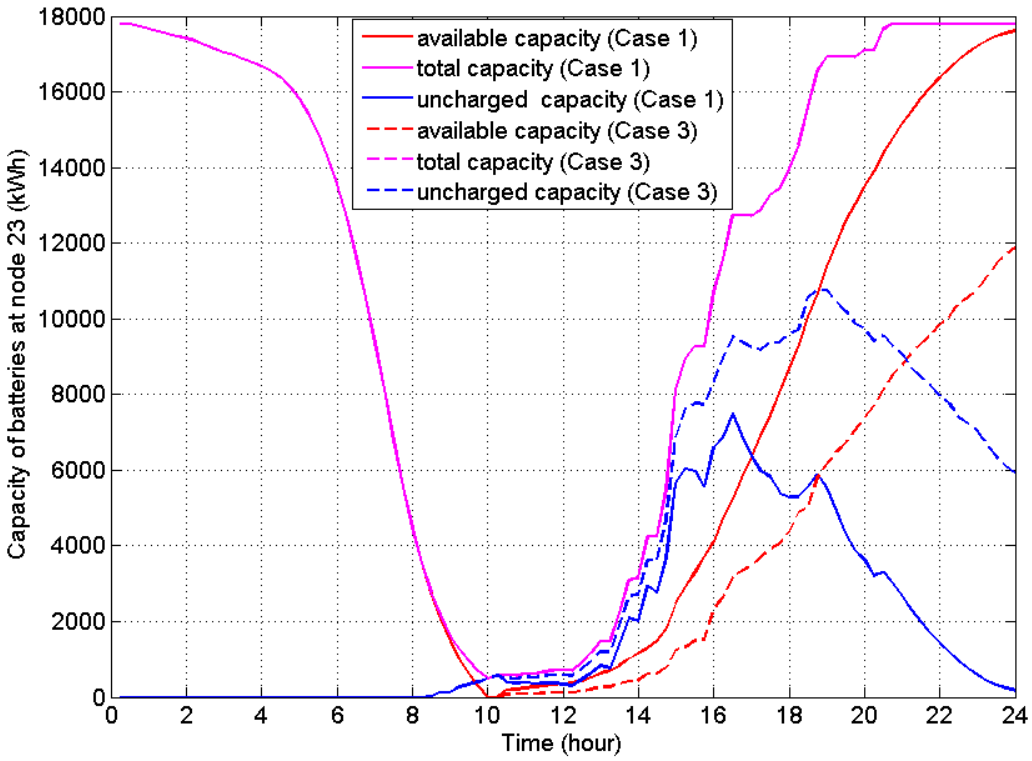

Figure 4.3. EV battery capacity at residential node 23 when no charging occurs at office

which is the total amount of battery capacities that can participate in V2G services. This amount is highest after 12 am in the case when EV charged with uncoordinated charging technique because most of the EVs that return from offices become fully charged at home by that time. During morning, uncharged battery capacities are zero because all EVs are fully charged. When EVs return to home from office during evening, their SOC decreases and uncharged battery capacities become available, however, they are connected to the grid for charging their batteries. At Node 23, very low batteries are uncharged until 12 am when uncoordinated charging technique is used. Uncharged batteries capacity are higher for the case using semi-coordinated charging technique (represented by dotted blue curve) since most of the batteries are charged after certain time delay in order to avoid coinciding with peak loads. Most of them are charged only after 12 am.

4.2.2 Capacity of EV batteries at commercial nodes when no charging occurs at office

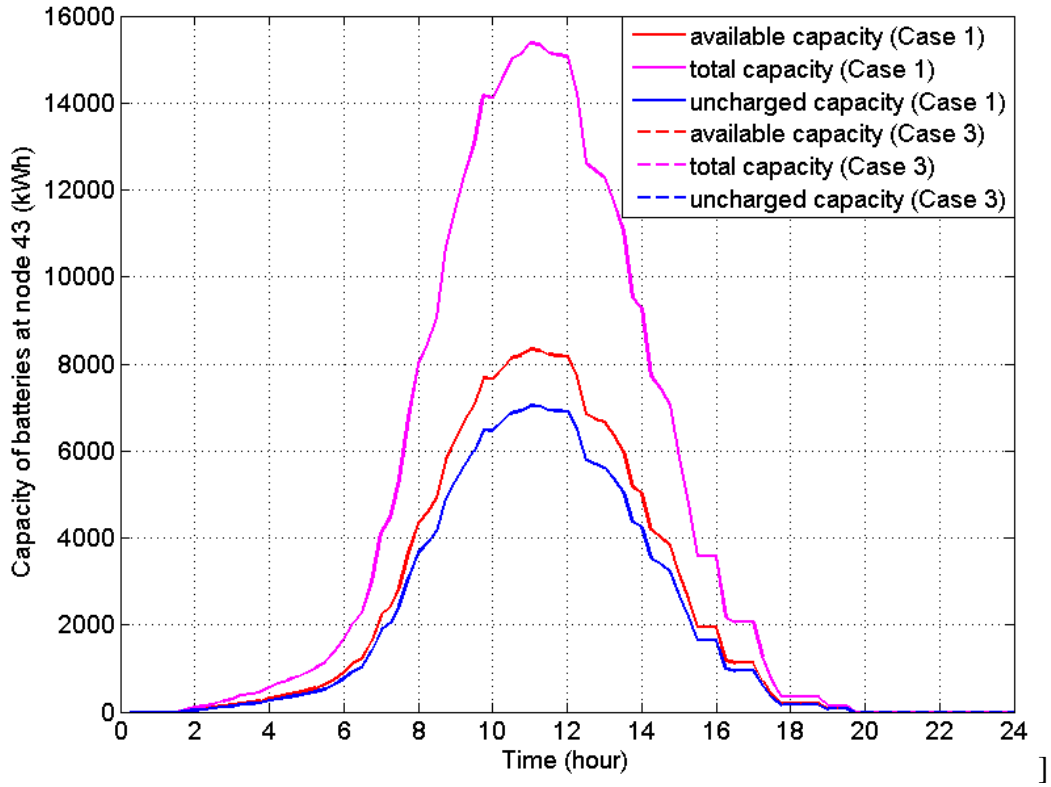

]

Figure 4.4. EV battery capacity at office node 43 when no charging occurs at office in the uncoordinated (Case 1) and semi-coordinated (Case3) cases.

Figure 4.4 shows the capacity of EV batteries available at office node 43 when EVs are charged only at home. The uncharged battery capacity are maximum from 10 am to 12 pm since most of the EVs are available at office during that time. The uncharged battery capacities at office due to uncoordinated and semi-coordinated charging overlap with each other because no EVs are charged at offices. The decrease in uncharged battery capacities at commercial node after 1 pm is due to the movement of EVs from office to residential areas at the end of the day.

4.2.3 Capacity of EV batteries at residential nodes when charging occurs at office

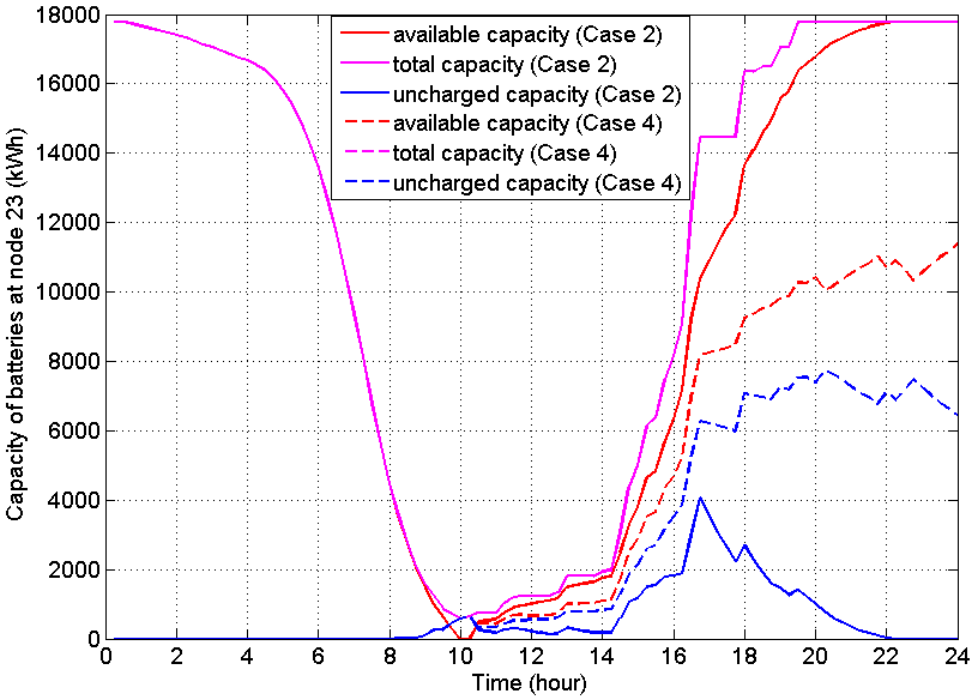

Figure 4.5. EV battery capacity at residential node 23 when charging occurs at office in the uncoordinated (Case 2) and semi-coordinated (Case 4) cases.

Figure 4.5 shows the capacity of EV batteries available at residential node 23 when EVs are charged at both home and offices. The pattern of graphs for uncoordinated charging is similar to those in Figure 4.3. The difference is that the capacity of batteries available for charging are lower as compared to the case when EVs are charged at home only. This is because EVs become fully charged while they are parked at the office (i.e., a full charge at the beginning of the trip from office to home). At residential node 23, all EVs become fully charged at 10 pm. The batteries need to be connected to the grid for shorter time in Case 2 as compared to Case 1. Red curves show the capacity of batteries at residential area that can participate in V2G services. These capacities are higher at

residential node in Case 2 as compared to Case 1. The uncharged battery capacities at residential nodes are higher for the Case 4 because EV loads are connected to grid for charging after certain time delay only. Hence, the capacity of batteries available for V2G service is lower for Case 4 as compared to Case 2.

4.2.4 Capacity of EV batteries at commercial nodes when charging occurs at office

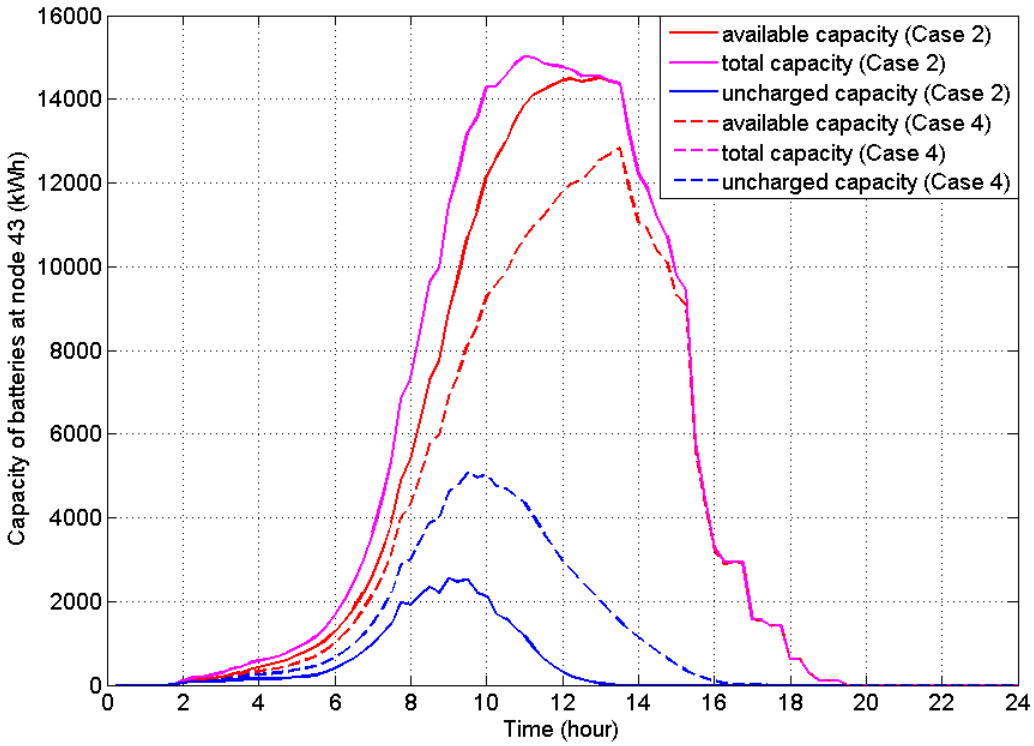

Figure 4.6. EV battery capacity at commercial node 43 when charging occurs at office in the uncoordinated (Case 2) and semi-coordinated (Case 4) cases.

Figure 4.6 shows the capacity of EV batteries available at office node 43 when EVs are charged at offices too. EVs are charged as soon as they arrive at office and all EVs become fully charged at 1 pm in Case 2 (represented by solid blue graph), but in Case 4, uncharged battery capacities are higher as compared to Case 2. All EVs become fully charged in Case 4 at 5 pm at office node 43. This is because EVs charging loads are

shifted uniformly throughout the parking duration so as to avoid larger EV charging during peak load periods. For V2G services, battery capacities available are higher in Case 2 as compared to Case 4. Uncharged battery capacities are zero after 8 pm because the number of EVs at office area is zero.

4.3 Temporal Distribution of Loads

The total load connected to each node of distribution system increases due to penetration of large number of EV charging loads. When no EVs are connected, total load is equal to the system load. EVs charging loads are much higher than the system load and are added to the system load .

4.3.1 Load connected to residential node when no charging occurs at office

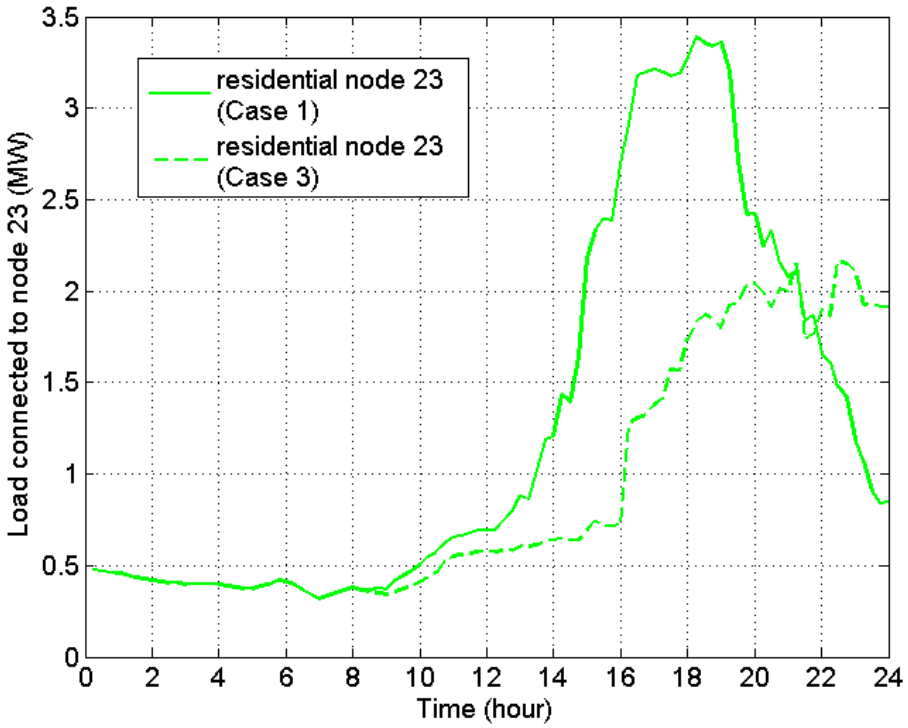

Figure 4.7. Load connected to a residential node 23 when no charging occurs at offices in the uncoordinated (Case 1) and semi-coordinated (Case3) cases.

Figure 4.7 shows the total load connected to the residential node 23 when EVs are charged at home only. Because EVs are not charged at offices, total loads connected to office nodes are equal to the system load connected to those nodes in Case 1 and Case 3. At residential node 23, peak loads are observed during the evening, i.e., from 4 pm to 7 pm due to uncoordinated charging of EVs. With semi-coordinated charging techniques, most of the EV charging loads are shifted to nighttime. During evening times, the load curve is flattened. The peak load for Case 1 decreased from 3.4 MW to 2.2 MW.

4.3.2 Load connected to residential and commercial node when charging occurs at office

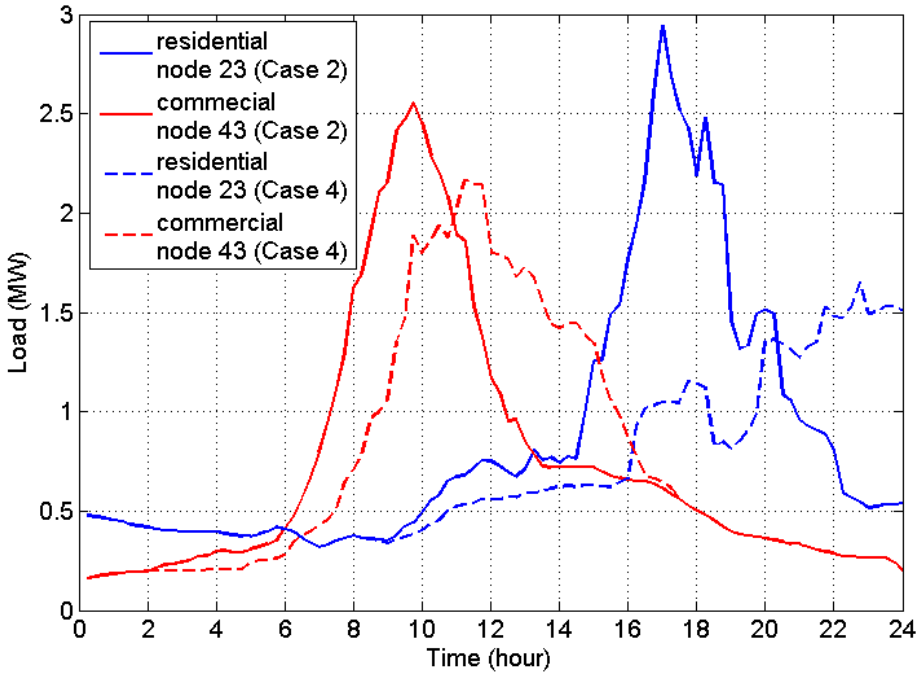

Figure 4.8. Load connected to a residential node 23 and commercial node 43 when charging occurs at offices in the uncoordinated (Case 2) and semi-coordinated (Case 4) cases.

Figure 4.8 shows the total load connected to the residential nodes 23 (blue curve) and office node 43 (red curve) when EVs are charged at both homes and offices. Due to charging of EVs at office nodes, the peak load at residential node 23 is reduced from 3.4

MW (Case 1) to 2.9 MW (Case 2). The peak load at office node 43 is increased from 0.74 MW (Case 1) to 2.6 MW (Case 2). Due to semi-coordinated charging, EV loads are shifted toward off-peak hours and peak load at Node 43 is reduced from 2.6 MW to 2.3 MW (Case 4) and the peak load at residential node 23 is reduced from 2.9 MW to 1.6 MW (Case 4). EV charging loads are uniformly distributed throughout parking duration at residential and commercial nodes in Case 4, while in Case 2 peaks are created in the system load. Hence, parking of EVs at office nodes cause shift in EV charging loads spatially and semi-coordinated charging technique cause shift in EV charging loads temporally.

4.4 Impact of EV charging load on node voltage for a single run case

Due to EV charging loads connected to the distribution network, voltage of various nodes of RBTS Bus 5 distribution system are affected. Uncoordinated charging technique exhibits under voltage issues on various nodes while semi-coordinated charging technique improves the voltage of affected buses. The voltage profile of one of the most affected residential and commercial nodes are explained in Section 4.4.1 and 4.4.2.

4.4.1 Voltage profile of residential nodes and commercial nodes when no EV charging occurs at office

Figure 4.9 shows the voltage at the residential node 23 when EVs are charged at home only. The cyan curve shows the voltage without any EVs connected and the solid green curve shows the voltage when EV loads are charged using the uncoordinated charging technique. The voltage drops below the allowable limit from 3:30 pm to 8 pm because most of the EVs are connected to Node 23 for charging during that time. In the

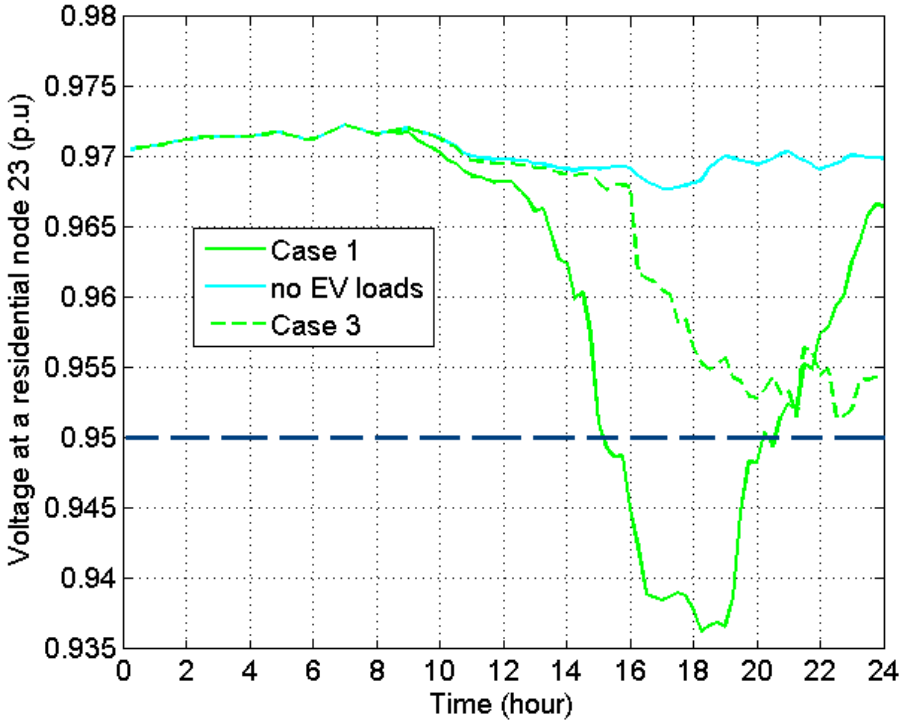

Figure 4.9. Voltage profile of residential node 23 for a day when no charging occurs at offices in the uncoordinated (Case 1) and semi-coordinated (Case 3) cases.

worst case, the voltage drops to 0.936 p.u. The dotted green curve shows the voltage using the semi-coordinated charging technique. In this case, the voltage drops to 0.952 p.u. in worst condition which lies within standard limit. This is due to the shifting of EV loads away from the peak load period.

Figure 4.10 shows the voltage at the commercial node 43 when EVs are charged at home only. The curves for all three cases overlap with each other because there is no EV charging load at office area. The voltage for all these cases lie within standard limit. The fluctuation in the voltage is due to the variation of system load at various time of the day.

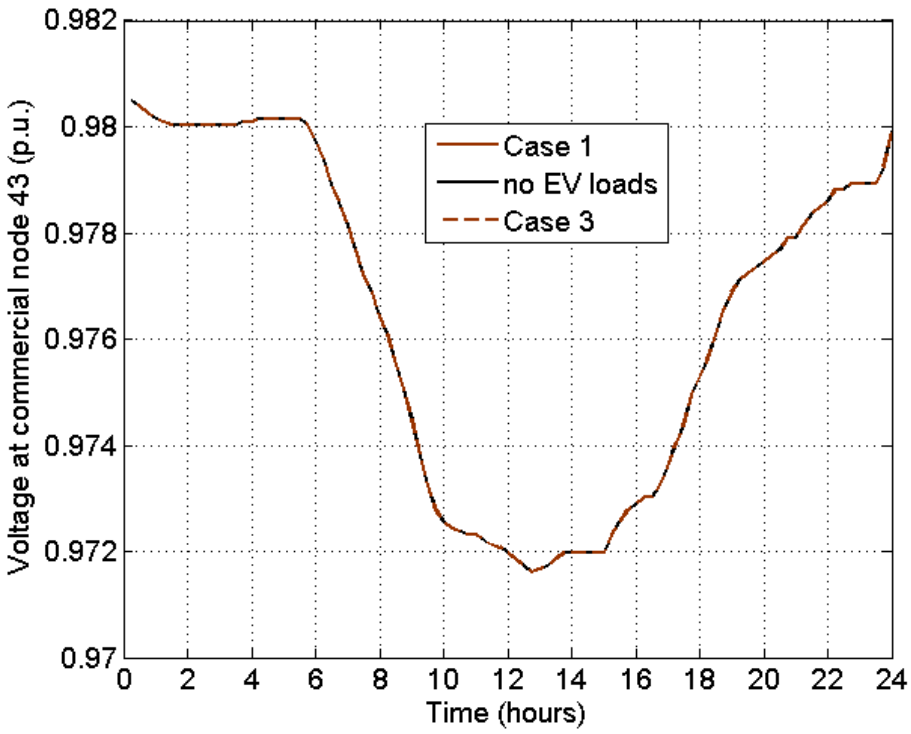

Figure 4.10. Voltage profile of commercial node 43 for a day when no charging occurs at offices in the uncoordinated (Case 1) and semi-coordinated (Case 3) cases.

4.4.2 Voltage profile of residential nodes and commercial nodes when charging occurs at offices

Figure 4.11 and 4.12 shows the voltage at residential node 23 and commercial node 43 when EVs are charged at both homes and offices. Due to load increment and decrement in office nodes and residential nodes, respectively, the voltage profile degraded in commercial nodes and improved in residential nodes in Case 2 as compared to Case 1. In Figure 4.11, solid blue curve shows that from 5 pm to 6:30 pm, the voltage at node 23 is below the standard limit. At worst condition, the minimum voltage is found to be 0.942 p.u. which is better as compared to Case 1. Even though the voltage profile is improved in Case 2, the voltage lies below permissible limits during the peak time. The voltage profile

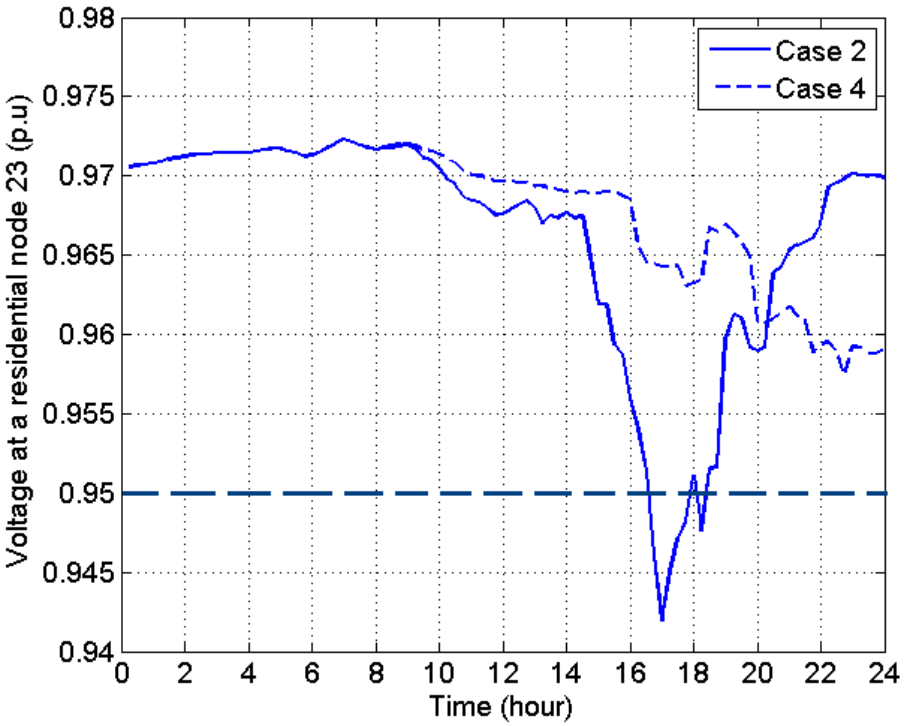

Figure 4.11. Voltage profile of residential node 23 for a day when charging occurs at offices in the uncoordinated (Case 2) and semi-coordinated (Case 4) cases.

is improved by introducing delays in the charging time (represented by the dotted blue curve). In Case 4, the minimum voltage is found to be 0.964 p.u, which lies within standard limit. As shown in Figure 4.12, at the office most of the EVs are charged between 9 am and 11 am (Case 2). The minimum voltage at node 43 reaches 0.946 p.u. due to uncontrolled charging (represented by solid red curve) and 0.95 p.u. due to semi-controlled charging method (represented by solid red curve in 4.12) which lies within limits.

4.5 Impact of EV charging load on node voltage using Monte Carlo simulation

To observe the effect of uncertainty related with driving behavior, the simulation is run multiple times using different values of driving speed and parking duration, i.e., performing Monte Carlo simulation. The possible range of voltage at various node of

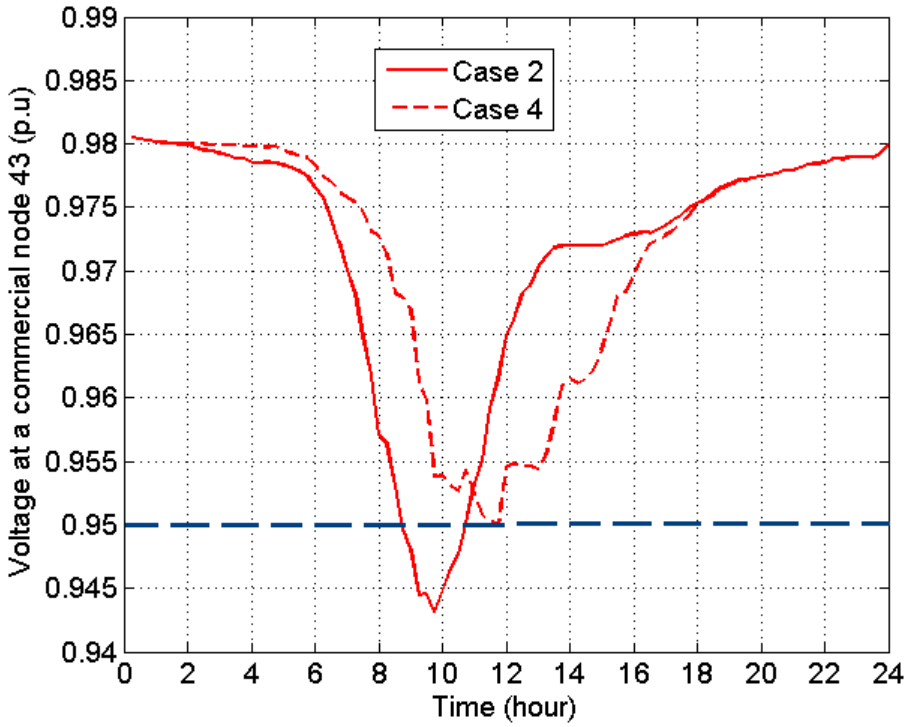

Figure 4.12. Voltage profile of commercial node 43 for a day when charging occurs at offices in the uncoordinated (Case 2) and semi-coordinated (Case 4) cases.

distribution network are determined. Figure 4.13– 4.15 give an overview of voltage profile during the worst case scenarios.

4.5.1 Voltage profile of residential nodes using Monte Carlo simulations when no charging occurs at office

Figure 4.13 shows the minimum and average voltage at residential node 23 when charging are performed at home only obtained over 50 Monte Carlo simulations. The minimum allowable limit is represented by the dotted straight line. The average voltage with uncoordinated charging technique (solid brown curve) drops below the standard limit, whereas the average voltage is within the standard limit using the semi-coordinated charging technique (solid green curve). However, the voltage due to semi-coordinated charging drops below standard limit during worst case scenarios (dotted green curve).

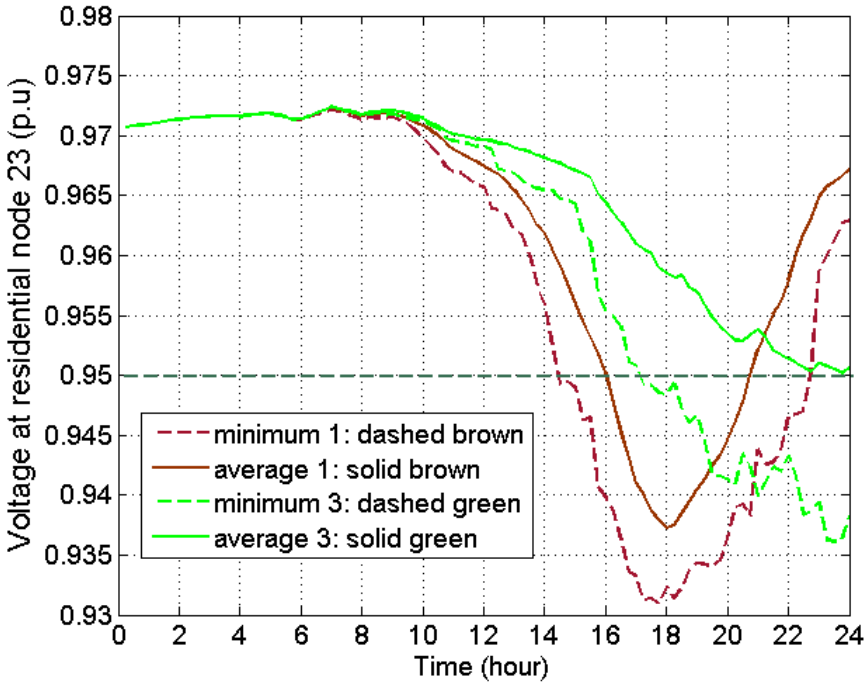

Figure 4.13. Voltage profile of residential node 23 obtained using Monte Carlo simulation when no charging occurs at offices in the uncoordinated (Case 1) and semi-coordinated (Case 3) cases.

4.5.2 Voltage profile of residential nodes and commercial nodes using Monte Carlo simulations when charging occurs at offices

Figure 4.14 show the minimum and average voltage at residential node 23 when charging are performed at both home and offices obtained over 50 Monte Carlo simulations. The average voltage lies slightly below the standard limit in Case 2 (solid magenta curve) as compared to Case 1. This is because EVs become fully charged at the office. Using the semi-coordinated charging technique, the average voltage lies within the allowable range (solid blue curve). However, the minimum voltage in Case 2 (dotted magenta curve) and Case 4 (dotted blue curve) lies below the standard limit. This is because of shifting charging EV loads within narrow time frame.

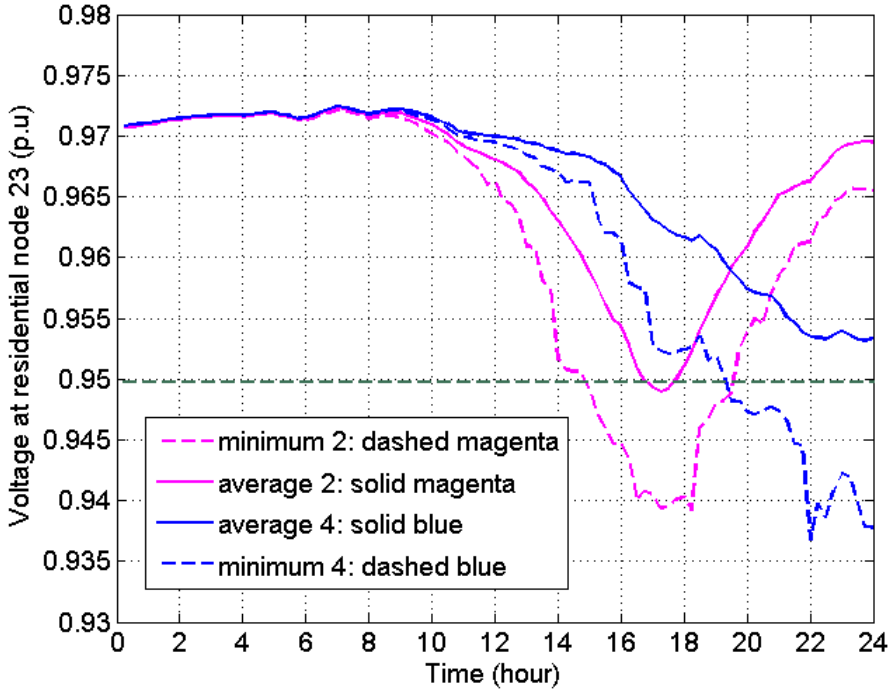

Figure 4.14. Voltage profile of residential node 23 obtained using Monte Carlo simulation when no charging occurs at offices in the uncoordinated (Case 2) and semi-coordinated (Case 4) cases.

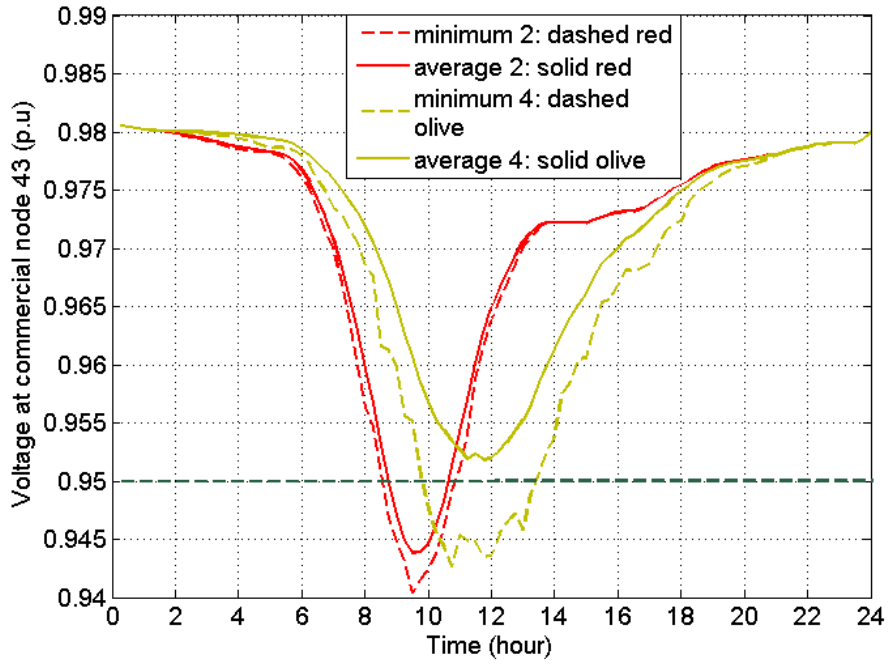

Figure 4.15. Voltage profile of commercial node 43 obtained using Monte Carlo simulation when no charging occurs at offices in the uncoordinated (Case 1) and semi-coordinated (Case 3) cases.

Figure 4.15 shows the minimum and average voltage at commercial node 43 when charging are performed at both home and offices obtained over 50 Monte Carlo simulations. Although the voltage at the residential node is improved, the average commercial node voltage dips below 0.95 p.u. during peak load hours in Case 2 (solid red curve). At Node 43, on average, voltage drop reaches up to 0.942 p.u. and 0.952 p.u. during peak load time in Case 2 and Case 4, respectively. With semi-coordinated charging, the average voltage lies above 0.95 p.u during the whole day. However, the voltage reaches to 0.944 p.u. during worst case with semi-coordinated charging technique.

CHAPTER 5 CONCLUSION

5.1 Summary

EVs will replace conventional combustion engine based vehicles to solve environmental and economic issues in the future. Higher penetration of EVs will cause negative impacts to the voltage and thermal limits of the power grid. Therefore, EV charging needs must be scheduled to reduce stress in the grid. For scheduling, it is important to determine the location of the EVs with respect to space (spatial) and time (temporal). Hence, a state transition algorithm was developed that determined the number of EVs available at any charging station at different time interval. Using this information, the total capacity of batteries available for charging and discharging at any charging station was determined. EV charging loads connected to any node can be calculated using information of number of EVs whose SOC is not 100 percent. However, the capacity of EV batteries available at any charging station depends on the randomness in driving behavior. There is also uncertainty related to the route EV users follow in traffic network. The decrease in SOC of EV battery is dependent on length of path EV travels in traffic system. Hence, detailed modeling of EVs in integrated traffic and power network is necessary.

EV batteries are charged when they are parked at any charging station. EV batteries are flexible loads whose charging can be shifted at different time of a day. Simulation results showed that the distribution networks are negatively affected when EVs are charged only at the end of the day using uncoordinated charging technique. The residential nodes with EVs will increase peak load demand that will cause voltage

problems in medium voltage distribution system. Hence, EV charging loads can be shifted towards commercial nodes to reduce the peak EV loads at residential nodes, but if EVs are charged at office areas with uncoordinated charging technique, EV charging time will coincide with peak load hours, exacerbating the peak demand. So, off-peak time charging need to be applied to maintain the voltage of medium voltage network within allowable limits. Therefore, the best way to mitigate voltage issues due to EV charging load is to shift them with respect to both time and position, i.e., use semi-coordinated charging method to charge EVs at both home and offices.

A model of EV was developed using the RBTS Bus 5 distribution system and traffic network developed by Tang et al. in [7]. The shortest distances between residential and commercial nodes were calculated by simulating EVs in the integrated traffic and power network. Randomness in driving behavior was added by considering speed and parking duration as normal distribution. End user driving pattern were obtained from NHTS. Slow chargers with charging rate of 3.3 kW were used to charge EVs. EV charging demand at different residential and commercial nodes were calculated in MATLAB using above information. Nodal voltage in power network were analyzed by adding EV charging load in nodes of RBTS Bus 5 system. The simulations were performed in MATPOWER to observe the voltage profile of nodes with EVs.

Simulation results showed that the load profile of the system was smoothened and the loading of the networks were reduced by using semi-coordinated charging techniques at home and office nodes. The voltage at residential and commercial nodes with EVs was improved to within permissible limits. This prevents the immediate need of additional transformers and other expensive equipment to solve voltage drop issues. Since this

method does not require any change in existing distribution system infrastructure, it can be considered as an inexpensive method. However, results from Monte Carlo simulations showed that even with the semi-coordinated charging method, the nodal voltage goes below allowable limit during worst case scenarios.

5.2 Conclusions

A state transition algorithm is suitable for determining the size of charging station based on number of EVs available at that charging station with respect to time and space. This algorithm can be used for any power system model with any number of residential and office areas combined with a traffic network. Randomness in driving behavior involves randomness in driving speed, parking duration and driving distance of EV users. Uncoordinated charging technique provides large charging demand to the power network that creates congestion in power system. EVs provide additional peak loads during morning and evening time at residential nodes and during afternoon at commercial nodes. A semi-coordinated charging technique shift EV charging loads towards off-peak hours and flattened the system load profile. This improves the voltage deviation in distribution network. This method is very useful for the planning and operation of distribution system, but sometimes due to randomness in driving behavior, semi-coordinated charging techniques cannot maintain the system voltage within the standard limit.

5.3 Future Work

In this thesis, the simulations are performed for a single day. However, simulations need to be done for longer time durations considering different system load profile for weekdays and weekends for better analysis. In the future, stochastic methods can be used

to forecast EV charging loads. Renewable energy sources, like solar and wind, should be added in the power system to charge EV batteries. Optimal use of available energy sources need to be done for charging EV batteries. Fully coordinated smart charging techniques that can provide maximum benefit to the customers can be applied. Different type of trip chain in a day, example, home to office to shopping center to home, home to school to office to school to home, etc. should be considered. Charging stations may be added in recreation areas using fast chargers. Information regarding capacity of batteries obtained using state transition algorithm can be used for power system restoration during blackout using EV batteries.

REFERENCES

[1] C. Brinson. (2012). How much air pollution comes from cars. Accessed: May 5, 2016, [Online]. Available: http://auto.howstuffworks.com/air-pollution-from-cars.html/.

[2] S. Deilami, A. S. Masoum, P. S. Moses, and M. A. S. Masoum, "Real-time coordination of plug-in electric vehicle charging in smart grids to minimize power losses and improve voltage profile," *IEEE Transactions on Smart Grid*, vol. 2, no. 3, pp. 456–467, 2011.

[3] T. Motors. (2011). Tesla unveils roadster 2.5 at newest stores in Europe and North-America. Accessed: May 10, 2016, [Online]. Available: https://www.teslamotors.com/about/press/releases/tesla-unveils-roadster-25-newest-stores-europe-and-north-america.

[4] K. Clement-Nyns, E. Haesen, and J. Driesen, "The impact of charging plug-in hybrid electric vehicles on a residential distribution grid," *IEEE Transactions on Power Systems*, vol. 25, no. 1, pp. 371–380, 2010.

[5] J. Taylor, A. Maitra, M. Alexander, D. Brooks, and M. Duvall, "Evaluations of plug-in electric vehicle distribution system impacts," in *IEEE PES General Meeting*, 2010, 6 pp.

[6] S. Huang and D. Infield, "The impact of domestic plug-in hybrid electric vehicles on power distribution system loads," in *2010 International Conference on Power System Technology (POWERCON)*, 2010, 7 pp.

[7] D. Tang and P. Wang, "Probabilistic modeling of nodal charging demand based on spatial-temporal dynamics of moving electric vehicles," *IEEE Transactions on Smart Grid*, vol. 7, no. 2, pp. 627–636, 2016.

[8] U.S. Department of Transportation, Federal Highway Administration, "2009 national household travel survey user's guide," Tech. Rep., 2011.

[9] A. Lojowska, D. Kurowicka, G. Papaefthymiou, and L. Sluis, "Stochastic modeling of power demand due to EVs using copula," *IEEE Transactions on Power Systems*, vol. 27, no. 4, pp. 1960–1968, 2012.

[10] K. Qian, C. Zhou, M. Allan, and Y. Yuan, "Load model for prediction of electric vehicle charging demand," in *2010 International Conference on Power System Technology (POWERCON)*, 2010, 6 pp.

[11] W. Liu, M. Zhang, B. Zeng, L. Wu, and J. Zhang, "Analyzing the impacts of electric vehicle charging on distribution system reliability," in *IEEE PES Innovative Smart Grid Technologies*, 2012, 6 pp.

[12] A. Simpson, "Cost-benefit analysis of plug-in hybrid electric vehicle technology," in *22nd International Battery, Hybrid and Fuel Cell Electric Vehicle Symposium and Exhibition (EVS-22)*, 2006, 12 pp.

[13] Electric Power Research Institute, "Environment assessment of plug-in hybrid electric vehicles," Tech. Rep., July, 2007.

[14] E. Akhavan-Rezai, M. F. Shaaban, E. F. El-Saadany, and A. Zidan, "Uncoordinated charging impacts of electric vehicles on electric distribution grids: Normal and fast charging comparison," in *2012 IEEE Power and Energy Society General Meeting*, 2012, 7 pp.

[15] L. P. Fernandez, T. G. Roman, R. Cossent, C. M. Domingo, and P. Frias, "Assessment of the impact of plug-in electric vehicles on distribution networks," *IEEE Transactions on Power Systems*, vol. 26, no. 1, pp. 206–213, 2011.

[16] J. Taylor, A. Maitra, M. Alexander, D. Brooks, and M. Duvall, "Evaluations of plug-in electric vehicle distribution system impacts," in *IEEE PES General Meeting*, 2010, 6 pp.

[17] T. K. Lee, Z. Bareket, T. Gordon, and Z. S. Filipi, "Stochastic modeling for studies of real-world PHEV usage: Driving schedule and daily temporal distributions," *IEEE Transactions on Vehicular Technology*, vol. 61, no. 4, pp. 1493–1502, 2012.

[18] Z. Shahan. (2015). Electric car evolution. accessed: May 6, 2016, [Online]. Available: http://cleantechnica.com/2015/04/26/electric-car-history/.

[19] A. Wilmoth. (2013). 40 percent of u.s. households could use electric vehicles. accessed: May 10, 2016, [Online]. Available: http://newsok.com/article/3913992.

[20] Simply Decoded. (2013). Smart grid technology : Decoded. accessed: May 6, 2016, [Online]. Available: http://www.simplydecoded.com/2013/06/28/smart-grid-technology-decoded/.

[21] P. Bossche, F. Vergels, J. Mierlo, J. Matheys, and W. Autenboer, "Subat: An assessment of sustainable battery technology," *Journal of power sources*, vol. 162, no. 2, pp. 913–919, 2006.

[22] R. G. Valle and J. Lopes, *Electric Vehicle Integration into Modern Power Networks*. NY, USA: Springer Science and Business Media, 2013.

[23] M. Alonso, A. Hortensia, G. Gardy, and J. Galan, "Optimal charging scheduling of electric vehicles in smart grids by heuristic algorithms," *Energies*, vol. 7, no. 4, pp. 2449–2475, 2014.

[24] E. Sortomme and M. A. El-Sharkawi, "Optimal scheduling of vehicle-to-grid energy and ancillary services," *IEEE Transactions on Smart Grid*, vol. 3, no. 1, pp. 351–359, 2012.

[25] E. Lakervi, E. Holmes, and I. of Electrical Engineers, *Electricity Distribution Network Design*. London, UK: Peter Pergrinus, 1995.

[26] A. Pansini, *Guide to Electrical Power Distribution Systems*. Lilburn, GA: Fairmont Press, 2005.

[27] R. Billinton and S. Jonnavithula, "A test system for teaching overall power system reliability assessment," *IEEE Transactions on Power Systems*, vol. 11, no. 4, pp. 1670–1676, 1996.

[28] S. Shrestha and T. M. Hansen, "Spatial-temporal stochasticity of electric vehicles in an integrated traffic and power system," in *IEEE International Conference on Electro/ Information Technology*, accepted, to appear, 2016.

[29] A. Dhamaniya and S. Chandra, "Speed characterstics of mixed traffic flow on urban arterials," *International Journal of Civil, Environmental, Structural, Construction and Architectural Engineering*, vol. 7, no. 11, pp. 883–888, 2013.

[30] Bobit Business Media. (2012). Some rural arkansas highways getting higher speed limits. Accessed: April 15, 2016, [Online]. Available: http://www.truckinginfo.com/news/story/2012/06/.

[31] PluginCars. (2015). Mitsubishi i-miev review. Accessed: April 18, 2016, [Online]. Available: http://www.plugincars.com/mitsubishi-i-miev.

[32] SAE International. (2011). SAE charging configurations and ratings terminology. Accessed: April 20, 2016, [Online]. Available: http://www.sae.org/smartgrid/chargingspeeds.pdf.

[33] U.S. Environmental Protection Agency and U.S. Department of Energy. (2013). Energy efficiency and renewable energy. Accessed: April 23, 2015, [Online]. Available: http://www.fueleconomy.gov/feg/evsbs.shtml.

[34] R. Walling and G. Shattuk, "Distribution transformer thermal behavior and aging in local delivery distribution system," in *19th International Conference on Electricity Distribution*, 2007, 4 pp.

[35] R. D. Zimmerman, C. E. Murillo-Sanchez, and R. J. Thomas, "MATPOWER: Steady-state operations, planning, and analysis tools for power systems research and education," *IEEE Transactions on Power Systems*, vol. 26, no. 1, pp. 12–19, 2011.